Please cite this article in press as: Gregory et al., A Link between RNA Metabolism and Silencing Affecting *Arabidopsis* Development, Developmental Cell (2008), doi:10.1016/j.devcel.2008.04.005

Developmental Cell
Article

A Link between RNA Metabolism and Silencing Affecting *Arabidopsis* Development

Brian D. Gregory,[1,2] Ronan C. O'Malley,[1,2] Ryan Lister,[1,2] Mark A. Urich,[1] Julian Tonti-Filippini,[3] Huaming Chen,[2] A. Harvey Millar,[3] and Joseph R. Ecker[1,2,*]
[1]Plant Biology Laboratory
[2]Genomic Analysis Laboratory
The Salk Institute for Biological Studies, La Jolla, CA 92037, USA
[3]ARC Centre of Excellence in Plant Energy Biology, The University of Western Australia, Crawley, WA 6009, Australia
*Correspondence: ecker@salk.edu
DOI 10.1016/j.devcel.2008.04.005

SUMMARY

MicroRNAs (miRNAs) and small interfering RNAs (siRNAs) are abundant endogenous small RNAs (smRNAs) that control transcript expression through posttranscriptional gene silencing. Here, we show that concomitant loss of XRN4/EIN5, a 5′-3′ exoribonuclease, and ABH1/CBP80, a subunit of the mRNA cap binding complex, results in *Arabidopsis* plants manifesting myriad developmental defects. We find that ABH1/CBP80 is necessary to obtain proper mature miRNA levels, which suggests this protein affects the miRNA-mediated RNA silencing pathway. Additionally, we show that XRN4/EIN5 affects the levels of a smRNA class that is processed from both sense and antisense strands of ~130 endogenous transcripts that apparently are converted to double-stranded RNA (dsRNA) and subsequently processed. We find that the parent transcripts of these smRNAs accumulate in an uncapped form upon loss of XRN4/EIN5, which suggests that uncapped endogenous transcripts can become smRNA biogenesis substrates. Overall, our results reveal unexpected connections between RNA metabolism and silencing pathways.

INTRODUCTION

RNA silencing represents a pathway that controls gene expression transcriptionally and posttranscriptionally (Baulcombe, 2004). In RNA silencing, production of double-stranded RNA (dsRNA) or self-complementary fold-back structures gives rise to small RNAs (smRNAs) through the activity of DICER or DICER-LIKE (DCL) RNase III-type ribonucleases (Jones-Rhoades et al., 2006). These smRNAs comprise the sequence-specific effectors of RNA silencing pathways that direct the negative regulation or control of genes, repetitive sequences, viruses, and mobile elements (Almeida and Allshire, 2005; Tomari and Zamore, 2005). In plants, these smRNAs are composed of microRNAs (miRNAs) and several classes of endogenous small interfering RNAs (siRNAs), which are differentiated from one another by their distinct biogenesis pathways and the classes of genomic loci from which they arise (Baulcombe, 2004).

miRNAs are a class of smRNAs that are 20–24 nucleotides in length and arise from much longer primary transcripts that form characteristic stem-loop structures (Bartel, 2004). In *Arabidopsis*, the stem-loop precursor of miRNAs is processed by DCL1 ribonuclease to generate a miRNA/miRNA* duplex with a 2 nucleotide (nt) 3′ overhang. The miRNA* is derived from the opposite strand of the stem-loop structure and pairs imperfectly with the miRNA (Bartel, 2004; Jones-Rhoades et al., 2006). The miRNA is then incorporated into an RNA-induced silencing complex (RISC) that has the ARGONAUTE1 (AGO1) protein at its core (Baumberger and Baulcombe, 2005; Qi et al., 2005).

Plant miRNAs have imperfect but extensive complementarity to their mRNA targets, and typically direct cleavage of these transcripts (Jones-Rhoades and Bartel, 2004; Llave et al., 2002). The targets of many plant miRNAs are mRNAs encoding transcription factors (Jones-Rhoades and Bartel, 2004), and the importance of miRNA-mediated regulation of a number of these target transcripts for proper development is well established (Mallory and Vaucheret, 2006; Willmann and Poethig, 2007). Additionally, plants containing mutations in genes encoding proteins involved in miRNA biogenesis or function (*AGO1*, *DCL1*, *HEN1*, *HYL1*, *SERRATE*, and *HST*) exhibit myriad dramatic developmental abnormalities, exemplifying the importance of this class of smRNAs in growth and differentiation (Boutet et al., 2003; Lobbes et al., 2006; Park et al., 2002; Prigge and Wagner, 2001; Vaucheret et al., 2004; Vazquez et al., 2004a; Yang et al., 2006).

Endogenous siRNAs are a class of smRNAs that arise from long dsRNA, which are formed as a product of an RNA-dependent RNA polymerase (RDR), by convergent transcription, or transcription of repetitive elements. siRNAs typically perform autosilencing, in that they target DNA or transcripts corresponding to (or homologous in sequence to) the loci from which they are processed (Baulcombe, 2004). However, the *trans*-acting siRNAs (tasiRNAs), which are processed from noncoding RNAs known as *TRANS-ACTING siRNA* (*TAS*) genes, are the exception in that they posttranscriptionally downregulate protein-coding transcripts from unrelated loci in a fashion reminiscent of the miRNA-directed RNA silencing pathway (Allen et al., 2005; Peragine et al., 2004; Vazquez et al., 2004b; Yoshikawa et al., 2005). During the biogenesis of tasiRNAs, a segment

Please cite this article in press as: Gregory et al., A Link between RNA Metabolism and Silencing Affecting *Arabidopsis* Development, Developmental Cell (2008), doi:10.1016/j.devcel.2008.04.005

of the *TAS* transcript that is defined by miRNA-mediated RISC cleavage is converted by RDR6 to dsRNA, which is successively cleaved by DCL4 into 21 nt siRNAs (Adenot et al., 2006; Allen et al., 2005; Fahlgren et al., 2006; Garcia et al., 2006).

Another class of plant endogenous siRNAs is the heterochromatic siRNAs, which are smRNAs that are mostly 24 nt in length and associated with DNA methylation. The concerted activity of plant-specific DNA-dependent RNA polymerases, PolIVa and PolIVb, correlates with the accumulation of 24 nt heterochromatic siRNAs via dsRNA formation by RDR2 and DCL3-mediated processing (Chan et al., 2005; Herr et al., 2005; Onodera et al., 2005; Xie et al., 2004). A fraction of these siRNAs associate with AGO4 to form a silencing complex thought to direct sequence-specific methylation events (Chan et al., 2005; Qi et al., 2006). Subsequently, this siRNA-directed DNA methylation can result in maintained transcriptional gene silencing at loci from which the smRNAs arise (Herr et al., 2005; Kanno et al., 2005; Onodera et al., 2005; Pontier et al., 2005).

The 5′ cap structure and the 3′ poly(A) tail are the two boundary marks that define the extreme borders of a eukaryotic mRNA. In the eukaryotic cell nucleus, the 5′ cap is recognized by the nuclear mRNA cap-binding complex (CBC). CBC is a heterodimeric complex that consists of a small (CBP20) and a large (CBP80) protein subunit (Mazza et al., 2001) that plays numerous roles in RNA metabolism (Aguilera, 2005). The *Arabidopsis* homolog of CBP80 is encoded by the *ABH1* gene. Plants harboring a genetic lesion in *ABH1* (*abh1-1* mutant plants) manifest an ABA-hypersensitive regulation of seed germination phenotype that suggests a link between mRNA metabolism and ABA signaling. Interestingly, the characterization of *abh1-1* mutant plants resulted in the discovery that *Arabidopsis* CBC is entirely composed of the ABH1/CBP80-AtCBP20 heteroduplex (Hugouvieux et al., 2001).

In *Arabidopsis*, the 5′-3′ exoribonuclease XRN4/EIN5 (henceforth referred to as EIN5) acts as an mRNA-degrading enzyme that is involved in the decay of specific transcripts that include the 3′ products of miRNA-mediated cleavage (Kastenmayer and Green, 2000; Souret et al., 2004). Two of its other mRNA targets, *EBF1* and *EBF2*, encode F box proteins that target the ubiquitin/proteasome-mediated turnover of EIN3, a key transcription factor mediating gene expression regulated by the phytohormone ethylene. These specific EIN5 targets account for the ethylene insensitive (Ein^{-}) phenotype exhibited by *ein5* mutant plants (Olmedo et al., 2006; Potuschak et al., 2006).

Here, through analysis of the developmental defects manifested on *ein5-6 abh1-1* double mutant plants, we demonstrate unexpected roles in RNA silencing pathways for two proteins involved in general RNA metabolism, ABH1/CBP80 (henceforth referred to ABH1) and EIN5. First, we find that loss of ABH1 decreases the levels of mature miRNAs, suggesting that this protein functions in the miRNA-mediated RNA silencing pathway. Additionally, we show that EIN5 affects the abundance of a distinct class of mostly 21 nt smRNAs that in many cases emanate from the entire length of endogenous functionally annotated transcripts, which often accumulate in an uncapped form in *ein5* mutant plants. Taken together, our results suggest that an additional fate for endogenous uncapped transcripts is shuttling into an RNA silencing pathway where they become smRNA-biogenesis substrates.

RESULTS

Ethylene Insensitivity of *ein5* Mutant Plants Is Suppressed by the *abh1* Mutation

The position that ABH1 occupies on mRNA molecules suggests that it may counteract the function of 5′-3′ exoribonucleases such as EIN5 (Aguilera, 2005). Therefore, in order to determine if mutation of *ABH1* can suppress the ethylene insensitivity of *ein5* mutant plants, we generated double mutants of *ein5* and *abh1*. We found that loss of ABH1 (*abh1-1*) almost completely suppresses the Ein^{-} phenotype of *ein5-6* mutant plants (Figures 1A–1E). Previously, we and others have demonstrated that the ethylene insensitivity of *ein5* mutant plants is a consequence of *EBF1* and *EBF2* mRNA accumulation (Olmedo et al., 2006; Potuschak et al., 2006). To characterize the effect of ABH1 on *EBF1* and *EBF2* mRNA levels, we performed northern blot analysis using total RNA from 3-day-old etiolated seedlings of wild-type Columbia (Col-0) ecotype, *abh1-1*, *ein5-6*, and *ein5-6 abh1-1* grown in hydrocarbon-free air or 10 parts per million (ppm) ethylene for various time periods (Figure 1F). We found that *abh1-1* seedlings maintained levels of *EBF1* and *EBF2* mRNA similar to those of wild-type Col-0 (Figure 1F). As expected, *ein5-6* seedlings accumulated a significantly increased level of both mRNAs in air and upon ethylene treatment (Figure 1F). Conversely, *ein5-6 abh1-1* seedlings exhibited levels of both *EBF1* and *EBF2* mRNA similar to those of wild-type Col-0 (Figure 1F), suggesting that loss of ABH1 restores proper maintenance of these two mRNAs in *ein5* mutant plants. Taken together, these results reveal that ABH1 is required for the accumulation of increased levels of *EBF1* and *EBF2* mRNAs in the absence of EIN5, and *abh1* mutation can act as a genetic suppressor of the hormone response phenotype manifested by *ein5* mutant plants.

ein5-6 abh1-1 Plants Manifest Developmental Defects Similar to Those Observed for miRNA Pathway Mutants

During analysis of the ethylene response of *ein5-6 abh1-1* mutant plants, we noticed they manifested severe developmental defects. Previously, *abh1-1* and *ein5-6* single mutant plants had been found to present a serrated leaf margin phenotype (Hugouvieux et al., 2002; Olmedo et al., 2006), which we have determined is strongly enhanced in *ein5-6 abh1-1* double mutant plants (Figure 2Q). In addition, a small percentage of *abh1-1* (~7%) and *ein5-6* (~1%) single mutant seedlings demonstrated fused cotyledons when compared with wild-type Col-0 plants, which never displayed this phenotype. This phenotype was also greatly enhanced in *ein5-6 abh1-1* double mutant seedlings, where we observed over 16% of seedlings with fused cotyledons (Figures 2A–2P). *ein5-6 abh1-1* double mutant flowers also manifested defects not observed for the other three genotypes, including extranumerary petals and bending of the gynoecium (Figure S1, see the Supplemental Data available with this article online). Finally, *abh1-1* and *ein5-6* single mutant plants were also found to manifest an altered phyllotactic pattern, where the internode length is severely decreased and results in multiple fruits emanating from the same node, which was observed at a far greater frequency in *ein5-6 abh1-1* double mutant plants (Figures 2R–2U). In fact, we observed numerous nodes from which more than three fruits emanated on double mutant plants, while

Please cite this article in press as: Gregory et al., A Link between RNA Metabolism and Silencing Affecting *Arabidopsis* Development, Developmental Cell (2008), doi:10.1016/j.devcel.2008.04.005

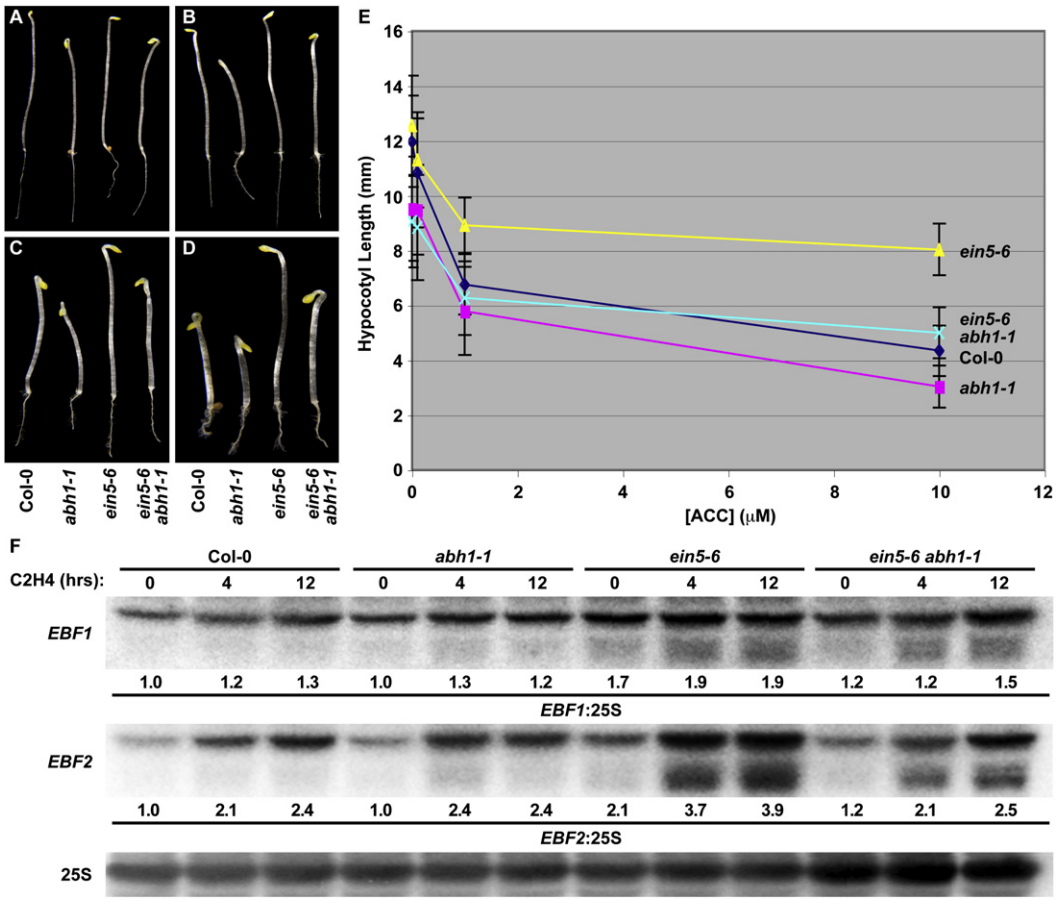

Figure 1. The Ethylene Insensitivity of *ein5* Mutant Plants Is Suppressed by *abh1* Mutation

(A–D) Triple-response phenotypes of wild-type Col-0, *abh1-1*, *ein5-6*, or *ein5-6 abh1-1* 3-day-old etiolated seedlings grown on LS medium without the ethylene precursor ACC (A), or with 0.1 μM (B), 1 μM (C), or 10 μM (D) ACC.

(E) Dosage response of 3-day-old etiolated seedlings of the indicated genotypes to various concentrations of ACC. Error bars, ± SD.

(F) Levels of *EBF1* and *EBF2* mRNA determined by northern analyses of total RNA from 3-day-old etiolated seedlings from the indicated genotypes grown in hydrocarbon-free air or treated for various times (indicated above wells) with 10 ppm ethylene (C2H4) gas using a 3′ probe to *EBF1* or *EBF2*. Twenty-five svedberg rRNA is shown as a loading control. Normalized values of *EBF1* and *EBF2* mRNA to rRNA control (Col-0 without ethylene treatment [0 hrs] set at 1.0) are indicated below the respective blot.

this phenotype was never manifested by plants of the other genotypes (Figure 2V). Interestingly, Prigge and Wagner (2001) previously determined that mutation of the *SERRATE* gene in *Arabidopsis* resulted in plants that presented similar phenotypes to those observed for *ein5-6 abh1-1*. Subsequently, it was determined that SERRATE is required for proper miRNA biogenesis (Lobbes et al., 2006; Yang et al., 2006). Therefore, the developmental defects manifested by *ein5-6 abh1-1* (and to a lesser extent *abh1-1* and *ein5-6*) suggested that loss of ABH1 and EIN5 might affect the miRNA-mediated RNA silencing pathway.

Loss of ABH1 and EIN5 Disrupts the miRNA-Mediated RNA Silencing Pathway

To determine if EIN5, ABH1, or both have effects on the miRNA-mediated RNA silencing pathway, we carried out an unbiased analysis of the transcriptome using whole-genome tiling microarrays (Chekanova et al., 2007; Kapranov et al., 2002; Figure S2 and Tables S1–S6). Interestingly, tiling microarray analysis revealed that the levels of a number of primary *MIRNA* transcripts were significantly increased in *ein5-6 abh1-1* (18 increased) and *abh1-1* (19 increased) compared with *ein5-6* and wild-type Col-0 plants (Figure 3A and Table S7). To establish that the stem-loop structure containing the miRNA/miRNA* duplex was part of the primary *MIRNA* transcript upregulated in our tiling array analysis and to provide validation for this class of mRNAs, we performed reverse transcription quantitative polymerase chain reaction (RT qPCR) with primer sets homologous to sequences just upstream and downstream of this structural moiety for a subset of the primary *MIRNA* transcripts that were statistically upregulated from our microarray studies (Table S7). We found that *ein5-6 abh1-1* and *abh1-1* mutant plants accumulated significantly more *MIRNA158a, MIRNA164b, MIRNA167a,* and *MIR168a* transcripts that contained the stem-loop structural moiety than did wild-type Col-0 or *ein5-6* plants (Figure 3B), suggesting that it is the loss of ABH1 that results in accumulation of this class of mRNAs (Figures 3A and 3B and Table S7).

Furthermore, tiling array analysis revealed that a number of miRNA-target mRNAs accumulated in *ein5-6 abh1-1* double

Please cite this article in press as: Gregory et al., A Link between RNA Metabolism and Silencing Affecting *Arabidopsis* Development, Developmental Cell (2008), doi:10.1016/j.devcel.2008.04.005

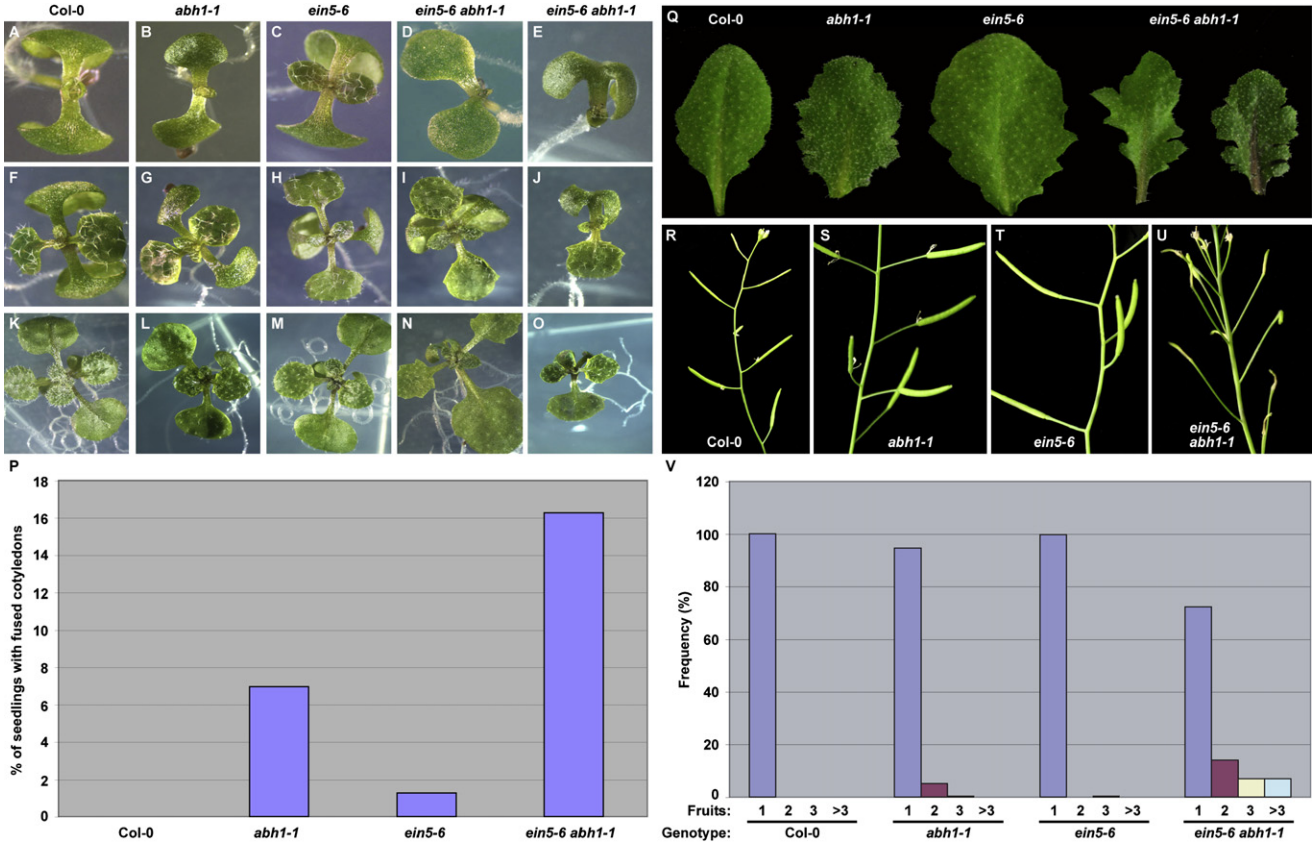

Figure 2. *ein5-6 abh1-1* Double Mutant Plants Manifest Developmental Defects Similar to Those Observed for miRNA Pathway Mutants

(A–E) One-week-old seedlings of wild-type Col-0 (A), *abh1-1* (B), *ein5-6* (C), and *ein5-6 abh1-1*, one of which manifests partial (D) and the other full (E) cotyledon fusion phenotypes.

(F–J) Ten-day-old seedlings of the same genotypes as in (A–E).

(K–O) Two-week-old seedlings of the same genotypes as in (A–E).

(P) The percentage of the seedlings of indicated genotype that manifest the cotyledon fusion defect, scored using 1-week-old plants.

(Q) Leaves of 5-week-old plants of the indicated genotypes. Both *ein5-6* and *abh1-1* single mutant plants have serrated leaf edges, which is strongly enhanced on *ein5-6 abh1-1* double mutant plants. The leaf margins of *ein5-6 abh1-1* double mutant plants are highly dentate and also often become asymmetric (left leaf) in their growth pattern.

(R–U) Inflorescence stems of the indicated genotypes.

(V) The percentage of the inflorescence stems of the indicated genotypes that manifest the developmental defect wherein multiple fruits (two, three, or more than three) emanate from the same node.

mutant plants to levels far exceeding those observed for the three other genotypes, two examples of which can be seen in Figure 3C (see also Table S5). We validated these two examples, *CUC1* and *HAP2C*, using RT qPCR (Figure 3D). As expected based on the tiling microarray results, we determined that *ein5-6 abh1-1* double mutant plants accumulated increased levels of the miRNA-target transcripts *CUC1* and *HAP2C* compared with the other three genotypes (Figure 3D). These results provided further validation of our tiling microarray analysis and suggest that the concomitant loss of ABH1 and EIN5 results in the accumulation of miRNA-target mRNAs. Previously, it was determined that these two classes of mRNAs (primary *MIRNA* transcripts and miRNA-target mRNAs) were significantly increased in *Arabidopsis* plants lacking proteins involved in miRNA biogenesis and function (Llave et al., 2002; Lobbes et al., 2006). Overall, these results suggest that concomitant loss of ABH1 and EIN5 disrupts miRNA-mediated RNA silencing.

ABH1 Affects the miRNA-Mediated RNA Silencing Pathway

Next, we wanted to obtain a genome-wide view of the effects of ABH1, EIN5, or both on the smRNA populations of *Arabidopsis*. In order to accomplish this, we employed deep sequencing of smRNA samples from wild-type Col-0, *abh1-1*, *ein5-6*, and *ein5-6 abh1-1* immature flower buds using an Illumina Genetic Analyzer (GA) (Figures S3 and S4). A total of 3,264,170 (1,036,593 unique), 4,446,687 (1,400,713 unique), 3,173,518 (1,030,343 unique), and 2,910,019 (959,915 unique) smRNAs were identified from the wild-type Col-0, *abh1-1*, *ein5-6*, and *ein5-6 abh1-1* sequencing libraries, respectively (Figure S4). We found that the majority (~86%) of smRNAs in all genotypes sequenced were 21–24 nt in size (data not shown). Upon focusing our analysis on the sequencing data encompassing the 21 nt size class of smRNAs, we noticed that this smRNA size class was overall underrepresented (~20%) in *abh1-1* single mutant

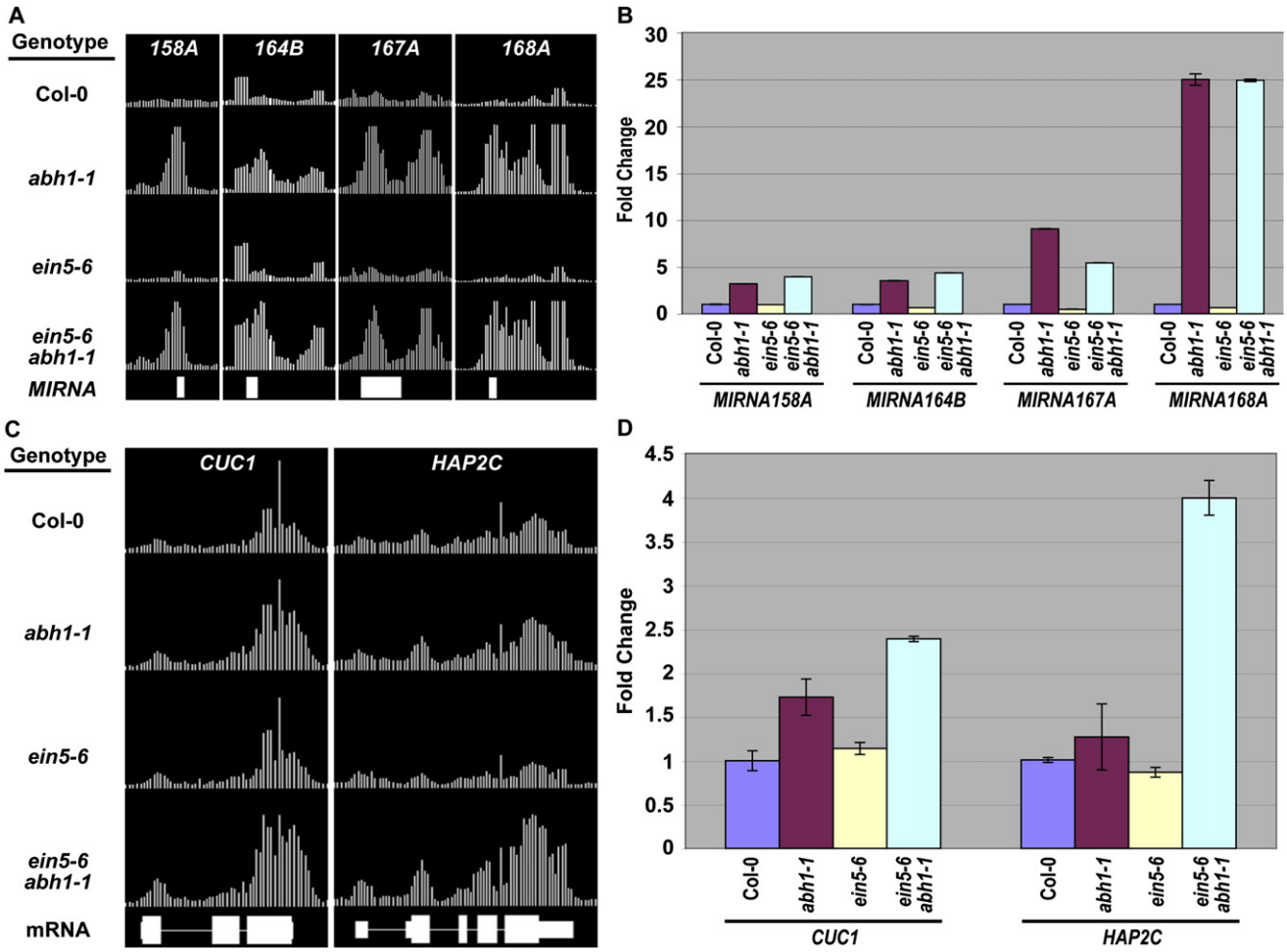

Figure 3. Tiling Microarray Analysis Suggests a Role for ABH1 and EIN5 in the miRNA-Mediated RNA Silencing Pathway

(A) The levels of primary *MIRNA158a, MIRNA164b, MIRNA167a,* and *MIRNA168a* mRNA were determined by *Arabidopsis* whole-genome tiling microarray expression analysis. The top four tracks display the level of primary *MIRNA* mRNAs in the indicated genotypes. The bottom track holds the annotated gene models for the primary *MIRNA* loci.

(B) Oligo(dT)-primed RT qPCR specific for the stem-loop region of primary *MIRNA158a, MIRNA164b, MIRNA167a,* and *MIRNA168a* mRNAs for wild-type Col-0 (blue bar), *abh1-1* (red bar), *ein5-6* (yellow bar), and *ein5-6 abh1-1* (light blue bar) plants. Error bars, ± SD.

(C) The levels of specific miRNA-target mRNAs, *CUC1* (*At3g15170*) and *HAP2C* (*At1g72830*), were determined by *Arabidopsis* whole-genome tiling microarray expression analysis. The top four tracks display the level of *CUC1* and *HAP2C* mRNAs in the indicated genotypes. The bottom track holds the annotated gene models for the *CUC1* and *HAP2C* loci.

(D) Oligo(dT)-primed RT qPCR analysis of *CUC1* and *HAP2C* mRNA levels. Error bars, ± SD.

plants compared with wild-type Col-0 (Figure S5A). These findings indicate that ABH1 is required to obtain proper levels of a class of smRNAs that are 21 nt in length. Conversely, we found that *ein5-6 abh1-1* double mutant plants accumulated higher levels of 21 nt smRNAs than the other three genotypes (Figure S5A), which suggests that EIN5 negatively regulates a class of 21 nt smRNAs. To obtain a genome-wide view of the 21 nt smRNA population, we first normalized the number of sequence reads at all genomic locations corresponding to 21 nt smRNAs by the total reads sequenced for the matching library, then parsed the values into 250 kilobase (kb) bins, and plotted these locations across the five *Arabidopsis* nuclear chromosomes. We found that for *abh1-1* and *ein5-6 abh1-1* plants, there was a reduction on average of ~60% in the levels of highly abundant 21 nt smRNAs, which correspond mostly to miRNAs (Figure 4A). These results suggest that ABH1 is required to obtain proper miRNA levels. Interestingly, we also observed that *ein5-6 abh1-1*, and to a lesser extent *ein5-6*, mutant plants accumulated 21 nt smRNA clusters that mapped to a number of different gene-rich locations throughout the *Arabidopsis* genome compared with the other two genotypes (Figure 4A, red arrows), suggesting that EIN5 negatively affects a population of 21 nt smRNAs (see below). To determine if these two proteins regulate the levels of specific classes of 21 nt smRNAs, we used our sequencing data encompassing another size class of smRNAs, 24 nts, as a control. This class of smRNAs has been demonstrated to consist mostly of heterochromatic siRNAs (Kasschau et al., 2007; Rajagopalan et al., 2006). We found that on

Please cite this article in press as: Gregory et al., A Link between RNA Metabolism and Silencing Affecting *Arabidopsis* Development, Developmental Cell (2008), doi:10.1016/j.devcel.2008.04.005

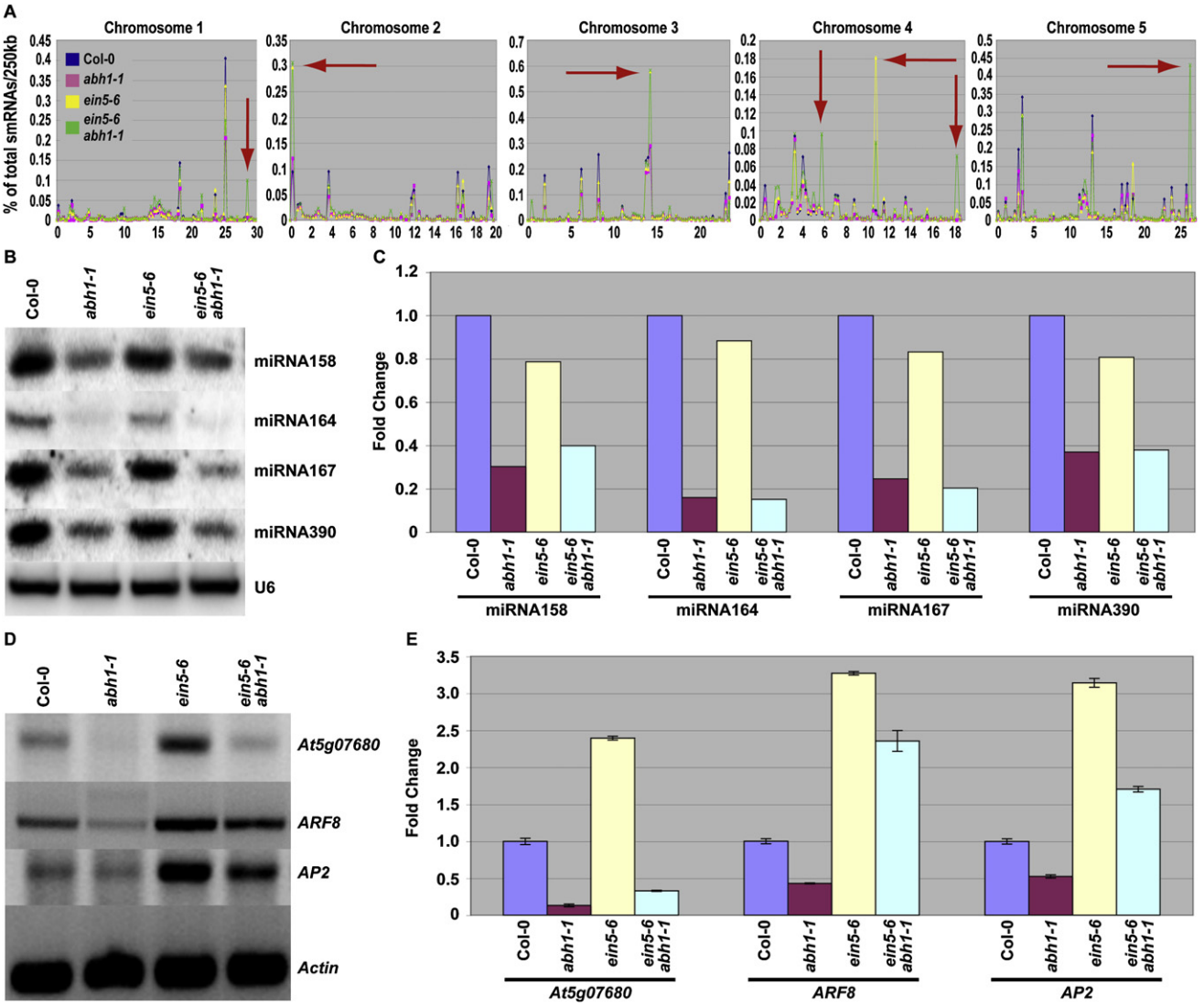

Figure 4. ABH1 Affects the miRNA-Mediated RNA Silencing Pathway

(A) Panels demonstrate the normalized abundance of 21 nt smRNAs (y axis, left-side scale) in a sliding 250 kb window in wild-type Col-0 (blue line), *abh1-1* (pink line), *ein5-6* (yellow line), and *ein5-6 abh1-1* (green line) double mutant plants. Red arrows indicate peaks of EIN5-affected smRNAs sequenced from *ein5-6* and *ein5-6 abh1-1* libraries.

(B) smRNA northern blot analysis of samples from indicated genotypes with DNA probes complementary to miRNA158, 164, 167, and 390. U6 is shown as a loading control.

(C) Normalized values of miRNA to the U6 control corresponding to three biological replicates for the indicated genotypes. The Col-0 value is set as 1.0.

(D) Agarose gel analyses of 5′-RACE products for *At5g07680*, *ARF8* (*At5g37020*), and *APETALA2* (*At4g36920*) miRNA-directed cleavage from the indicated genotypes. Actin was used as a loading control for the 5′-RACE experiments.

(E) Oligo(dT)-primed RT qPCR analysis of 5′-RACE products for *At5g07680*, *ARF8* (*At5g37020*), and *APETALA2* (*At4g36920*) miRNA-directed cleavage from the indicated genotypes. Error bars, ± SD.

a genome-wide scale, the levels of 24 nt smRNAs were not significantly different between the four sequenced genotypes (Figure S5B), indicating that EIN5 and ABH1 specifically regulated certain classes of 21 nt smRNAs.

To validate our sequencing data and further characterize ABH1's effect on miRNA levels, we performed smRNA-enriched northern blot analysis on samples from wild-type Col-0, *abh1-1, ein5-6*, and *ein5-6 abh1-1* immature flower buds. These experiments revealed that *abh1-1* and *ein5-6 abh1-1* plants accumulated 62%–83% less miRNA for all those interrogated (miRNA156, 158, 159, 164, 167, 169, and 390) compared with wild-type Col-0 and *ein5-6* (Figures 4B and 4C and Figure S6). Furthermore, this reduction in the levels of miRNAs upon loss of ABH1 function was corroborated by our smRNA sequencing data when the number of reads for specific miRNAs was normalized to the total sequenced read numbers (Figure S7A). Taken together, these results suggest that ABH1 is required to obtain proper miRNA levels. Notably, the smRNA sequencing data

demonstrated that the normalized levels of some well-characterized 24 nt siRNAs were not reduced by the loss of ABH1 function (Figure S7B), which suggests that this protein is specific in its effect on miRNA levels.

To test if the reduction in miRNA levels observed for *abh1-1* and *ein5-6 abh1-1* plants affected miRNA-mediated target mRNA cleavage, we employed a modified 5′-rapid amplification of cDNA ends (5′-RACE) protocol (Llave et al., 2002). Using this methodology we found that for *abh1-1* and *ein5-6 abh1-1* plants, there was decreased miRNA-mediated cleavage of the target mRNAs interrogated compared with those of wild-type Col-0 and *ein5-6* (Figures 4D and 4E). Overall, these results demonstrate that ABH1 is required to obtain wild-type levels of miRNAs, and suggest it has effects on the miRNA-mediated RNA silencing pathway through the reduction of this class of smRNA.

Next, we wanted to determine if mutation of *ABH1* could enhance the developmental defects manifested by plants containing a hypomorphic allele of *AGO1*, because AGO1 is known to function in the miRNA-mediated RNA silencing pathway. To do this, we generated double mutants between *abh1-8* (a null allele) and plants containing a hypomorphic allele of *AGO1*, *ago1-38*. A hypomorphic allele of *AGO1* was used because plants harboring null mutations in this gene do not survive. We then analyzed the *abh1-8 ago1-38* double mutant plants for novel growth defects or enhancement of developmental abnormalities manifested in *abh1-8* or *ago1-38* single mutant plants (Figure 5). We found that approximately 15% of *abh1-8 ago1-38* double mutant seedlings exhibited fused cotyledons, which was more than double the amount manifested by either *abh1-8* or *ago1-38* single mutant plants (Figures 5B–5E, 5G–5J, 5L–5O, and 5P). Furthermore, none of the wild-type Col-0 seedlings analyzed exhibited this developmental abnormality (Figures 5A and 5P). Additionally, we found that approximately 12% of *abh1-8 ago1-38* double mutant seedlings never developed a root, even after 2 weeks of growth (Figures 5E, 5J, 5O, and 5Q). Interestingly, this developmental defect was never observed for wild-type Col-0, *abh1-8*, or *ago1-38* single mutant plants (Figures 5A–5C, 5F–5H, 5K–5M, and 5Q). We also found that *abh1-8 ago1-38* double mutant plants presented an enhancement of the altered phyllotaxy wherein the internode length is severely decreased, resulting in multiple fruits emanating from the same node, as also demonstrated by both *abh1-8* and *ago1-38* single mutant plants. Specifically, ~16% of all *abh1-8 ago1-38* double mutant plants manifested more than three fruits emanating from the same node, which is more than double the amount witnessed for wild-type Col-0, *abh1-8*, or *ago1-38* single mutant plants (Figures 5R and 5S). These results demonstrate that the *abh1-8* mutation is able to enhance the developmental defects manifested by *Arabidopsis* plants harboring a hypomorphic mutant allele of *AGO1*, which suggests that like AGO1, ABH1 also affects the miRNA-mediated RNA silencing pathway.

EIN5 Affects the Levels of a Class of smRNAs Processed from Functionally Annotated mRNAs

As noted previously, we observed that in the absence of EIN5 function, clusters of 21 nt smRNAs accumulate in euchromatic regions of the genome (Figure 4A). Therefore, we filtered the sequenced smRNAs for 21 nt smRNAs present at least twice in *abh1-1*, *ein5-6*, or *ein5-6 abh1-1*, but not found in Col-0. These three lists were further filtered for functionally annotated mRNAs from which at least two independent smRNAs were processed, which identified 67, 253, and 235 such transcripts from *abh1-1*, *ein5-6*, and *ein5-6 abh1-1* plants, respectively (Figure 6A and Tables S8–S10). We found that 156 of these transcripts overlap between the *ein5-6* and *ein5-6 abh1-1* lists, with 23 of them also overlapping with those found for *abh1-1* (Table S11). Since the smRNAs observed (Figure 4A) were only present in the absence of EIN5, we focused on the 133 transcripts that overlapped between the lists from the *ein5-6* and *ein5-6 abh1-1* smRNA libraries (Figure 6A, Tables S11 and S12). We found that clusters of mostly 21 nt smRNAs were generated from both sense and antisense strands of these 133 functionally annotated transcripts (Figures 6B and 6C), suggesting that these mRNAs had been converted to dsRNA and then processed in 21 nt increments in the absence of functional EIN5 (Figures 6B and 6C). In many cases, these EIN5-affected smRNAs are processed from the entire length of the parental transcript in multiple 21 nt registers, which suggests there is not an ordered processing event or "common" mRNA terminus that is consistently required for biogenesis of these smRNAs (Figure 6B and Figure S8). There were also numerous examples where the EIN5-affected smRNAs accumulated to significantly higher levels in *ein5-6 abh1-1* compared with *ein5-6* plants (Figures 6B and 6D, Figure S9, and Table S12). In fact, these smRNAs compose ~19% of the entire 21 nt smRNA population of *ein5-6 abh1-1* double mutant plants (Figure S10), which suggests that concomitant loss of ABH1 and EIN5 results in the enhanced processing or stability (or both) of these smRNAs. Interestingly, we observed that often low levels of EIN5-affected smRNAs were present in wild-type plants (Figures 6B and 6D, Figure S9, and Table S12), which indicates that this class of smRNAs is indeed processed under normal conditions and is not just a byproduct of unnatural consequences (i.e. *ein5* mutation). Overall, these results suggest that the 5′-3′ ribonuclease EIN5 negatively regulates the levels of a class of endogenous smRNAs that are processed from functionally annotated *Arabidopsis* gene transcripts.

Endogenous Uncapped Transcripts Likely Act as smRNA Biogenesis Substrates

It had been previously reported that EIN5 likely antagonizes RDR-dependent RNA silencing of exogenously introduced transgenes through degradation of "aberrant" mRNAs that may lack a 5′ terminal cap moiety and serve as biogenesis substrates for smRNA production (Gazzani et al., 2004). Many of the features exhibited by our endogenous EIN5-affected smRNA-generating transcripts (Figure 6) suggest that they may also lack a 5′ terminal cap moiety, and therefore are regulated in a similar manner to what was previously witnessed for transgene mRNAs. To detect uncapped 5′ RNA ends, we used a modified 5′-RACE protocol (Llave et al., 2002). Full-length, decapped mRNA corresponding to the EIN5-affected smRNA-generating transcripts (verified by cloning and sequencing of the cDNA; Figure S11) consistently accumulated in *ein5-6* and *ein5-6 abh1-1* plants (Figure 7A). In order to generate a more comprehensive, genome-wide view of all 133 smRNA-generating transcripts, we designed an Illumina GA sequencing-based 5′-RACE assay termed *g*enome-wide *m*apping of *u*ncapped

Please cite this article in press as: Gregory et al., A Link between RNA Metabolism and Silencing Affecting *Arabidopsis* Development, Developmental Cell (2008), doi:10.1016/j.devcel.2008.04.005

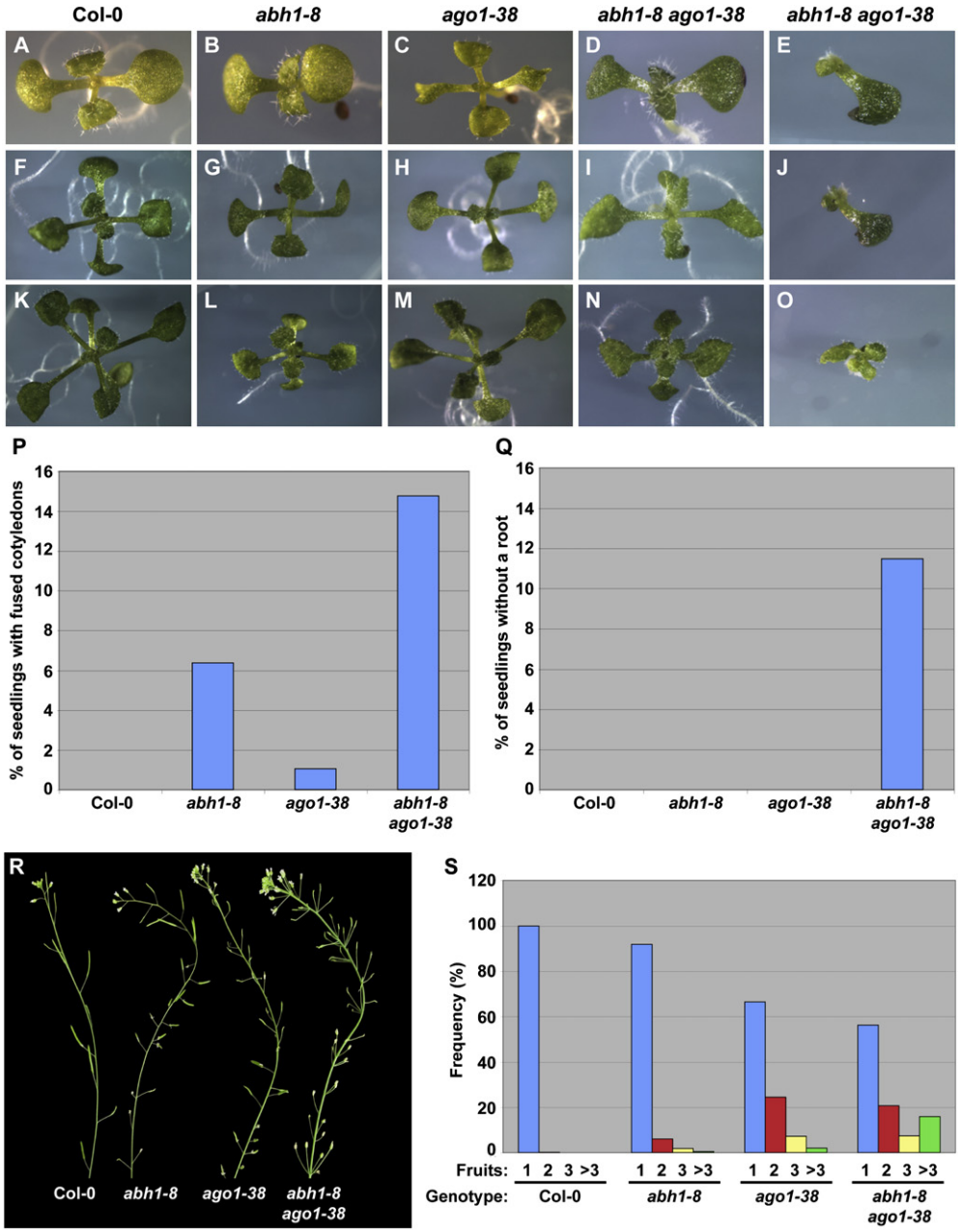

Figure 5. The *abh1* Mutation Enhances Developmental Defects Associated with Plants Containing a Hypomorphic Genetic Lesion in *AGO1*, *ago1-38*

(A–E) One-week-old seedlings of wild-type Col-0 (A), *abh1-8* (B), *ago1-38* (C), and *abh1-8 ago1-38* (D and E) double mutant plants, the latter of which manifests a cotyledon fusion phenotype and has no root (E).

(F–J) Ten-day-old seedlings of the same genotypes as in (A–E).

(K–O) Two-week-old seedlings of the same genotypes as in (A–E).

(P) The percentage of wild-type Col-0, *abh1-8*, *ago1-38*, and *abh1-8 ago1-38* double mutant seedlings that manifest the cotyledon fusion defect, which was scored using 1-week-old plants.

(Q) The percentage of wild-type Col-0, *abh1-8*, *ago1-38*, and *abh1-8 ago1-38* double mutant seedlings that do not develop a root, which was scored using 2-week-old plants.

(R) Inflorescence stems of plants of the indicated genotypes.

(S) The percentage of wild-type Col-0, *abh1-8*, *ago1-38*, and *abh1-8 ago1-38* double mutant inflorescence stems that manifest the developmental defect wherein multiple fruits (two, three, or more than three) emanate from the same node.

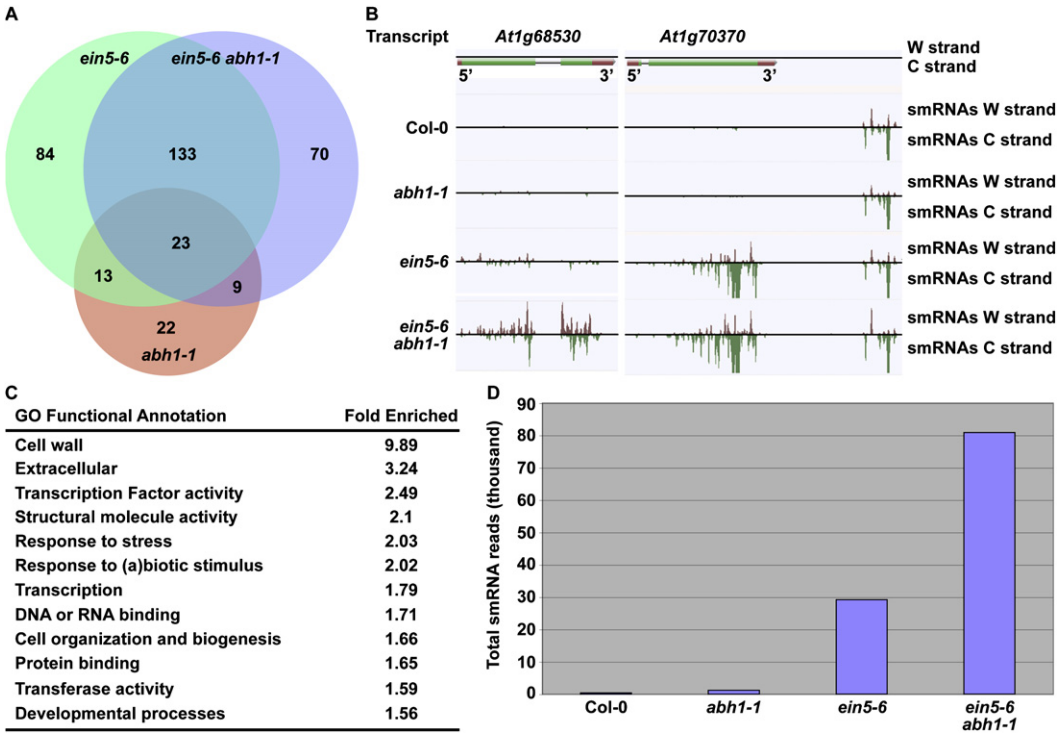

GO Functional Annotation	Fold Enriched
Cell wall	9.89
Extracellular	3.24
Transcription Factor activity	2.49
Structural molecule activity	2.1
Response to stress	2.03
Response to (a)biotic stimulus	2.02
Transcription	1.79
DNA or RNA binding	1.71
Cell organization and biogenesis	1.66
Protein binding	1.65
Transferase activity	1.59
Developmental processes	1.56

Figure 6. Clusters of EIN5-Affected smRNAs That Emanate from Functionally Annotated Endogenous Transcripts

(A) Venn diagram representation of annotated transcripts from which multiple 21 nt smRNAs were sequenced at least twice in the case of *abh1-1*, *ein5-6*, and *ein5-6 abh1-1* double mutant plants, but never for wild-type Col-0.

(B) Two examples of EIN5-affected 21 nt smRNA-generating transcripts (screenshots from the smRNAome database, http://neomorph.salk.edu/aj_salk/smRNAome.html). W (red bars) and C (green bars) indicate the signal from Watson and Crick strands, respectively.

(C) Table of Gene Ontology (GO) functional annotations that are over-represented by at least 1.5-fold for the 133 transcripts from which the EIN5-affected smRNAs are processed compared with the Col-0 reference transcriptome.

(D) The total number of smRNA sequence reads that correspond to EIN5-affected smRNAs from the wild-type Col-0, *abh1-1*, *ein5-6*, and *ein5-6 abh1-1* libraries, which was determined using the data in Table S12.

and *c*leaved *t*ranscripts (GMUCT) (see Figure S12 and Experimental Procedures for details). We then applied GMUCT to unmodified, poly-adenylated RNA samples from wild-type Col-0 and *ein5-6* immature flower buds. As expected for this modified 5′-RACE protocol, we were able to identify known miRNA-mediated target mRNA cleavage sites from the obtained sequencing data (Figure S13), thereby providing validation of this methodology. Using this novel assay we determined that at least 46% of the EIN5-affected siRNA-generating transcripts accumulate in an uncapped form in the absence of EIN5 function (Figures 7B and 7C). Overall, we validated ~50% of the total population of EIN5-affected smRNA-generating transcripts as accumulating in an uncapped form in *ein5-6* mutant plants through the combination of 5′-RACE and GMUCT (Figure 7B), with two of these mRNAs being validated by both methodologies. These results demonstrate that EIN5 is responsible for the removal of the uncapped forms of these 133 transcripts. Thus, we have identified a class of endogenous EIN5-affected mRNAs that are processed into smRNAs by an RNA silencing pathway similar to one previously observed to regulate aberrant transgenic RNAs (Gazzani et al., 2004; Figure 7). More specifically, the endogenous mRNAs also accumulate in an uncapped form, which is likely the defining feature that shunts them into an RNA silencing pathway where they are processed into mostly 21 nt smRNAs.

DISCUSSION

The mRNA CBC is known to increase the efficiency of pre-mRNA splicing and non-sense-mediated decay (NMD) (an mRNA surveillance pathway that generally eliminates messenger RNAs that prematurely terminate translation) through direct interaction with proteins involved in these two important processes (Aguilera, 2005). Therefore, we hypothesize that because ABH1 is a subunit of the CBC, its role in the miRNA-mediated mRNA silencing pathway could be to increase the efficiency of processing of these smRNAs from the initial primary *MIRNA* transcript. Specifically, we suggest that CBC bound to the 5′ end of primary *MIRNA* transcripts interacts with one of the proteins of the miRNA biogenesis complex (SERRATE, DCL1, and/or HYL1), thus increasing the likelihood of proper processing of these important smRNAs. The overlapping phenotypic similarities between *abh1* and *se* mutant plants (Bezerra et al., 2004; Figure 2 and Figure 5) offer a tantalizing suggestion that ABH1 may interact directly with SERRATE to ensure proper and efficient processing of primary *MIRNA* transcripts into the biologically active miRNA products.

Interestingly, consistent with our findings and providing evidence that a role for ABH1 in the miRNA-mediated RNA silencing pathway may also be conserved in animals, Parry et al. (2007)

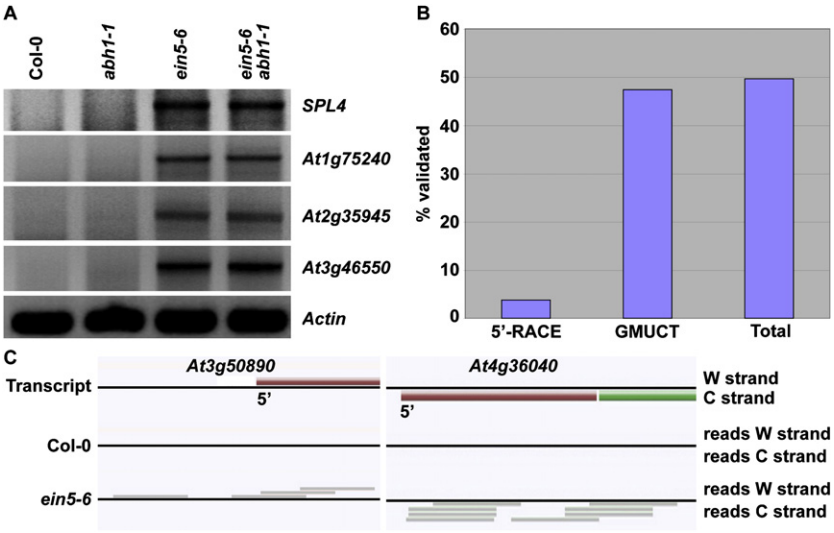

Figure 7. Transcripts from which EIN5-Affected smRNAs Are Processed Accumulate in an Uncapped Form

(A) 5′-RACE products of *SPL4*, *At1g75240*, *At2g35945*, and *At3g46550* corresponding to decapped (free 5′ terminal phosphate) versions of the indicated transcripts, which can only be detected in *ein5-6* and *ein5-6 abh1-1* samples. Actin was used as a loading control.

(B) The percent of EIN5-affected smRNA-generating transcripts validated as accumulating in an uncapped form by 5′-RACE, GMUCT, or both.

(C) Two examples of uncapped EIN5-affected smRNA-generating transcripts (screenshots from the smRNAome database) that were validated by the GMUCT method. W and C indicate the signal from Watson and Crick strands, respectively. Gray bars represent independent Illumina sequencing reads.

recently performed a whole-genome RNA interference (RNAi) screen in *C. elegans* that suggested a function for the worm homolog of ABH1 (F37E3.1) specifically in the *let-7* miRNA-mediated RNA silencing pathway. Upon performing smRNA northern blots using RNA isolated from young adult worms that were fed an RNAi knockdown construct targeting F37E3.1, only a slight reduction in mature *let-7* levels compared with those of wild-type animals was detected. Based on these results, this group concluded that the miRNA-debilitating gene inactivation of F37E3.1 likely abrogated gene function downstream of the expression and processing of *let-7*. But here, we demonstrate that *Arabidopsis* ABH1 is intimately required for accumulation of mature miRNA levels, which suggests a role for this protein either in or upstream of miRNA processing. These discrepancies may result from differences in the miRNA biogenesis pathways between the two organisms (*C. elegans* and *Arabidopsis*) examined in these studies, or more likely are due to differences in methodologies employed: RNAi knockdown (Parry et al., 2007) versus stable genetic mutation (*abh1* mutant plants [this study]). The latter suggestion is supported by the fact that even complete and stable loss of ABH1 in *Arabidopsis* caused an ~66% reduction in mature miRNA levels, rather than a complete loss (Figure 4 and Figures S6 and S7). Therefore, transient and incomplete reduction of F37E3.1 levels by RNAi likely only causes a slight decrease in mature miRNA levels, which would result in the differing interpretations of the results. Nevertheless, in combination these studies suggest an unexpected role for ABH1 in the miRNA-mediated RNA silencing pathway of eukaryotic organisms.

Additionally, we demonstrate that EIN5 affects the levels of a class of mostly 21 nt smRNAs that are processed from functionally annotated *Arabidopsis* gene transcripts (Figure 6). We find that the smRNA-generating mRNAs accumulate in an uncapped form in the absence of EIN5 function (Figure 7), which suggests that this may be the defining feature of these transcripts that shuttles them into an RNA silencing pathway, much like was previously demonstrated to occur for capless mRNAs derived from introduced transgenes (Gazzani et al., 2004). An alternative hypothesis would be that loss of EIN5 function allows cryptic antisense transcripts specific to the 133 EIN5-affected smRNA-generating loci to accumulate, thereby resulting in dsRNA formation and subsequent DICER processing into smRNAs. We strongly disfavor this latter hypothesis because our tiling microarray analysis did not reveal upregulated antisense transcripts corresponding to any of the 133 EIN5-affected smRNA-generating loci. Additionally, none of the EIN5-affected smRNAs map to the intronic regions of transcripts from which they are processed (Figure 6B), which strongly suggests that the mature mRNA molecule itself is acting as the template for synthesis of the antisense strand, likely in an RDR-dependent manner. Furthermore, we observe an enhancement in the levels of many of the EIN5-affected smRNAs in *ein5-6 abh1-1* double mutant plants compared with those of any of the other three genotypes used in this study (Figures 6B and 6D, Figure S9, and Table S12), which suggests that the processing and/or stability of these smRNAs is enhanced by the absence of both ABH1 and EIN5 function. While these results led us to prefer the latter explanation, wherein enhanced processing of the EIN5-affected smRNAs results from an increased availability of their biogenesis substrate, these models are not mutually exclusive. Specifically, based on the data from the *ein5-6 abh1-1* double mutant, we hypothesize that the loss of ABH1 function likely reduces protection of the 5′ cap structure from removal by decapping enzymes, while at the same time, the lack of functional EIN5 stabilizes these uncapped RNA intermediates. Overall, these results support a model in which the 133 transcripts that accumulate in an uncapped form in the absence of EIN5 function are shunted into an RDR-dependent RNA silencing pathway where they are processed into smRNAs. Furthermore, the findings presented herein for the single and double mutants suggest an integration of EIN5 and ABH1 functions in protecting these 133 endogenous transcripts from this proposed fate.

Recently, it was demonstrated that the terminal 5′ nucleotide of *Arabidopsis* smRNAs specifies the AGO protein with which they associate. Specifically, it was found that smRNAs with a 5′ terminal adenosine preferentially associate with AGO2 and AGO4, smRNAs with a 5′ terminal cytosine preferentially associate with AGO5, and smRNAs with a 5′ terminal uridine

preferentially associate with AGO1 (Mi et al., 2008). From deep smRNA sequencing, we find that the majority of 21 nt smRNAs from immature flower buds begin with a 5′ adenosine (Figure S14 and Table S13), and this is also observed for the entire population of sequenced smRNAs (data not shown). Therefore, the majority of smRNAs in these plant organs associate with AGO2 and AGO4. Guanine is the next most abundant 5′ terminal nucleotide for 21 nt smRNAs, while thymine and cytosine are the least favored 5′ terminal nucleotides for 21 nt smRNAs (Figure S14 and Table S13). Interestingly, the distribution of 5′ terminal nucleotides among the 21 nt EIN5-affected smRNAs is not significantly different from that in the total population of 21 nt smRNAs (Figure S14 and Table S13). Overall, these results suggest that EIN5-affected smRNAs are quite diversified at the 5′ terminal nucleotide position, which likely allows them to associate with a number of different *Arabidopsis* AGO proteins.

As noted above, we observed numerous cases of EIN5-affected smRNAs that correspond to gene transcripts that are also detectable in wild-type plants (Figures 6B and 6D, Figure S9, and Table S12), which indicates that the processing of this class of smRNAs is not simply a byproduct of genetic mutation of *EIN5* and *ABH1*. An intriguing possibility is that these smRNAs may have regulatory functions, and that they might be processed more readily and/or accumulate in response to specific physiological or environmental conditions in which the function of EIN5 is negatively regulated. In this model, the expansion of EIN5-affected smRNAs could thus provide an additional population of smRNAs to regulate target mRNAs with sites of sequence complementarity in both *cis* and *trans*. Although evidence that EIN5-affected smRNAs are able to regulate mRNAs posttranscriptionally is still lacking, this tantalizing possibility warrants further examination. Overall, these findings suggest that there is still much to learn concerning RNA silencing and the regulation of these posttranscriptional regulatory pathways.

EXPERIMENTAL PROCEDURES

Plant Materials

The Col-0 ecotype of *Arabidopsis* was used in this study. The *abh1-1* and *ein5-6* mutants were previously identified (Hugouvieux et al., 2001, 2002; Olmedo et al., 2006). *abh1-8* (this study) was recovered from the Salk T-DNA collection (Alonso et al., 2003). *ago1-38* comes from an ethyl methanesulfonate (EMS)-mutagenized population, and contains a Gly to Arg substitution at position 186 (seeds kindly provided by E. Meyerowitz, California Institute of Technology).

Genetic Analysis of Double Mutants

Double mutant plants were generated by genetic crosses, and homozygous lines were identified by PCR-based genotyping. All primers used for PCR-based genotyping of mutant plants used in this study can be found in Table S14. In the case of *ein5-6* genotyping, the amplified PCR products were subsequently cleaved with MboII. In the case of *ago1-38* genotyping, the amplified PCR products were subsequently cleaved with EcoNI.

RNA Analyses

For all experiments performed herein, immature flower bud clusters were collected for RNA isolation using the RNeasy Plant Mini Kit (QIAGEN, Valencia, CA). Low-molecular-weight RNA was purified from total RNA, and northern blots for mature miRNAs were performed as previously described (Peragine et al., 2004). Northern blot analysis of *EBF1* and *EBF2* mRNA levels was performed as previously described (Olmedo et al., 2006). Transcripts were quantified by RT qPCR using the comparative threshold cycle method ($\Delta\Delta C_t$, primers listed in Table S14), using *Actin 2* (*At3g18780*) as the endogenous reference.

5′-RACE

5′-RACE and cloning of 5′-RACE products was carried out using the GeneRacer Kit (Invitrogen, Carlsbad, CA) as previously described (Kasschau et al., 2003). Briefly, there were no modifications made to the total RNA used for the 5′-RACE experiments. The 5′-adaptor molecule was immediately ligated onto the total RNA population, thereby isolating only mRNAs or mRNA fragments with a 5′ end with a free 5′ phosphate. 5′-RACE products of miRNA-directed cleavage (Figure S7) were quantified by RT qPCR using the comparative threshold cycle method ($\Delta\Delta C_t$, primers listed in Table S14), using *Actin 2* (*At3g18780*) as the endogenous reference.

Microarray Analysis

Tiling microarray analysis was carried out as previously described (Chekanova et al., 2007). For more detailed methodology see the Supplemental Experimental Procedures.

smRNA Library Construction

smRNA libraries were constructed as per the manufacturer's instructions (Illumina Inc., San Diego, CA). For more detailed methodology see the Supplemental Experimental Procedures and Figure S3.

GMUCT Sequencing Library Construction

Briefly, GMUCT libraries were constructed by adapting a modified 5′-RACE protocol (see 5′-RACE section above) for sequencing on an Illumina GA. For more detailed methodology see the Supplemental Experimental Procedures and Figure S12.

High-Throughput Sequencing

smRNA and GMUCT libraries were sequenced using the Illumina GA as per the manufacturer's instructions (Illumina Inc., San Diego, CA), except that sequencing of GMUCT libraries was performed for 50 cycles to yield longer sequences that are more amenable to unambiguous mapping to the *Arabidopsis* genome sequence.

Mapping smRNA Reads

Sequence information was extracted from the image files with the Illumina Firecrest and Bustard software applications. Prior to alignment of the smRNA reads, a custom Perl script was used to identify the first seven bases of the 3′ adaptor sequence, and the read was truncated up to the junction with the adaptor sequence. No further analysis was performed on reads that did not contain adaptor sequence, as those reads lacking an adaptor cannot be precisely sized. The reads were then mapped to the *Arabidopsis* Col-0 reference genome (TAIR v.7) with the Illumina Eland application. Eland aligns 32 base pair or shorter reads with up to two mismatches to a reference genome. However, only perfect matches were excepted because shorter reads have a higher tendency to falsely map than longer reads. Since Eland does not return positions for reads that map to multiple positions in the reference genome, we utilized the Basic Local Alignment Search Tool (BLAST) to map these nonunique reads, using a word size of 10 and expectation value of 10. Once again, only perfect matches were accepted, because these shorter reads have a higher tendency to falsely map than longer reads.

Mapping GMUCT Reads

In order to avoid omitting reads mapping within unannotated transcripts, 36 base sequence reads were aligned to the *Arabidopsis* reference genome sequence (TAIR v.7) with the Eland application.

ACCESSION NUMBERS

All raw microarray data (CEL files) for expression analyses (wild-type Col-0, *abh1-1*, *ein5-6*, and *ein5-6 abh1-1*), as well as smRNA (Col-0, *abh1-1*, *ein5-6*, and *ein5-6 abh1-1* libraries) and GMUCT (wild-type Col-0 and *ein5-6* libraries) sequence data from our analyses, were deposited in Gene Expression Omnibus under the accession GSE11070.

Please cite this article in press as: Gregory et al., A Link between RNA Metabolism and Silencing Affecting *Arabidopsis* Development, Developmental Cell (2008), doi:10.1016/j.devcel.2008.04.005

SUPPLEMENTAL DATA

The Supplemental Data include fourteen figures, fourteen tables, Supplemental Experimental Procedures, and Supplemental References and can be found with this article online at http://www.developmentalcell.org/cgi/content/full/14/6/■■■/DC1/.

ACKNOWLEDGMENTS

The authors thank Angelita C. Garcia for technical assistance; Kim Emerson for assistance with preparing digital artwork; and Jennifer C. Fletcher, Eva C. Ziegelhoffer, and Elliot M. Meyerowitz for *ago1-38* seeds. B.D.G. is a Damon Runyon Fellow supported by the Damon Runyon Cancer Research Foundation (DRG-1909-06). R.L. is supported by a Human Frontier Science Program Long-term Fellowship. J.T.-F. is supported by Hackett and Shacklock Scholarships from the University of Western Australia. The development of the visualization and genome profiling browser AnnoJ was supported by grants from the Australian Research Council to A.H.M. (CE0561495 and DP0771156). This work was supported by grants from the NSF (MCB-0516888) and DOE (DE-FG02-04ER15517) to J.R.E.

Received: March 7, 2008
Revised: April 1, 2008
Accepted: April 23, 2008
Published online: May 15, 2008

REFERENCES

Adenot, X., Elmayan, T., Lauressergues, D., Boutet, S., Bouche, N., Gasciolli, V., and Vaucheret, H. (2006). DRB4-dependent TAS3 trans-acting siRNAs control leaf morphology through AGO7. Curr. Biol. *16*, 927–932.

Aguilera, A. (2005). Cotranscriptional mRNP assembly: from the DNA to the nuclear pore. Curr. Opin. Cell Biol. *17*, 242–250.

Allen, E., Xie, Z., Gustafson, A.M., and Carrington, J.C. (2005). microRNA-directed phasing during trans-acting siRNA biogenesis in plants. Cell *121*, 207–221.

Almeida, R., and Allshire, R.C. (2005). RNA silencing and genome regulation. Trends Cell Biol. *15*, 251–258.

Alonso, J.M., Stepanova, A.N., Leisse, T.J., Kim, C.J., Chen, H., Shinn, P., Stevenson, D.K., Zimmerman, J., Barajas, P., Cheuk, R., et al. (2003). Genome-wide insertional mutagenesis of *Arabidopsis thaliana*. Science *301*, 653–657.

Bartel, D.P. (2004). MicroRNAs: genomics, biogenesis, mechanism, and function. Cell *116*, 281–297.

Baulcombe, D. (2004). RNA silencing in plants. Nature *431*, 356–363.

Baumberger, N., and Baulcombe, D.C. (2005). Arabidopsis ARGONAUTE1 is an RNA Slicer that selectively recruits microRNAs and short interfering RNAs. Proc. Natl. Acad. Sci. USA *102*, 11928–11933.

Bezerra, I.C., Michaels, S.D., Schomburg, F.M., and Amasino, R.M. (2004). Lesions in the mRNA cap-binding gene ABA HYPERSENSITIVE 1 suppress FRIGIDA-mediated delayed flowering in *Arabidopsis*. Plant J. *40*, 112–119.

Boutet, S., Vazquez, F., Liu, J., Beclin, C., Fagard, M., Gratias, A., Morel, J.B., Crete, P., Chen, X., and Vaucheret, H. (2003). *Arabidopsis* HEN1: a genetic link between endogenous miRNA controlling development and siRNA controlling transgene silencing and virus resistance. Curr. Biol. *13*, 843–848.

Chan, S.W., Henderson, I.R., and Jacobsen, S.E. (2005). Gardening the genome: DNA methylation in *Arabidopsis thaliana*. Nat. Rev. Genet. *6*, 351–360.

Chekanova, J.A., Gregory, B.D., Reverdatto, S.V., Chen, H., Kumar, R., Hooker, T., Yazaki, J., Li, P., Skiba, N., Peng, Q., et al. (2007). Genome-wide high-resolution mapping of exosome substrates reveals hidden features in the *Arabidopsis* transcriptome. Cell *131*, 1340–1353.

Fahlgren, N., Montgomery, T.A., Howell, M.D., Allen, E., Dvorak, S.K., Alexander, A.L., and Carrington, J.C. (2006). Regulation of AUXIN RESPONSE FACTOR3 by TAS3 ta-siRNA affects developmental timing and patterning in *Arabidopsis*. Curr. Biol. *16*, 939–944.

Garcia, D., Collier, S.A., Byrne, M.E., and Martienssen, R.A. (2006). Specification of leaf polarity in *Arabidopsis* via the trans-acting siRNA pathway. Curr. Biol. *16*, 933–938.

Gazzani, S., Lawrenson, T., Woodward, C., Headon, D., and Sablowski, R. (2004). A link between mRNA turnover and RNA interference in *Arabidopsis*. Science *306*, 1046–1048.

Herr, A.J., Jensen, M.B., Dalmay, T., and Baulcombe, D.C. (2005). RNA polymerase IV directs silencing of endogenous DNA. Science *308*, 118–120.

Hugouvieux, V., Kwak, J.M., and Schroeder, J.I. (2001). An mRNA cap binding protein, ABH1, modulates early abscisic acid signal transduction in *Arabidopsis*. Cell *106*, 477–487.

Hugouvieux, V., Murata, Y., Young, J.J., Kwak, J.M., Mackesy, D.Z., and Schroeder, J.I. (2002). Localization, ion channel regulation, and genetic interactions during abscisic acid signaling of the nuclear mRNA cap-binding protein, ABH1. Plant Physiol. *130*, 1276–1287.

Jones-Rhoades, M.W., and Bartel, D.P. (2004). Computational identification of plant microRNAs and their targets, including a stress-induced miRNA. Mol. Cell *14*, 787–799.

Jones-Rhoades, M.W., Bartel, D.P., and Bartel, B. (2006). MicroRNAS and their regulatory roles in plants. Annu. Rev. Plant Biol. *57*, 19–53.

Kanno, T., Huettel, B., Mette, M.F., Aufsatz, W., Jaligot, E., Daxinger, L., Kreil, D.P., Matzke, M., and Matzke, A.J. (2005). Atypical RNA polymerase subunits required for RNA-directed DNA methylation. Nat. Genet. *37*, 761–765.

Kapranov, P., Cawley, S.E., Drenkow, J., Bekiranov, S., Strausberg, R.L., Fodor, S.P., and Gingeras, T.R. (2002). Large-scale transcriptional activity in chromosomes 21 and 22. Science *296*, 916–919.

Kasschau, K.D., Fahlgren, N., Chapman, E.J., Sullivan, C.M., Cumbie, J.S., Givan, S.A., and Carrington, J.C. (2007). Genome-wide profiling and analysis of *Arabidopsis* siRNAs. PLoS Biol. *5*, e57. 10.1371/journal.pbio.0050057.

Kasschau, K.D., Xie, Z., Allen, E., Llave, C., Chapman, E.J., Krizan, K.A., and Carrington, J.C. (2003). P1/HC-Pro, a viral suppressor of RNA silencing, interferes with *Arabidopsis* development and miRNA unction. Dev. Cell *4*, 205–217.

Kastenmayer, J.P., and Green, P.J. (2000). Novel features of the XRN-family in *Arabidopsis*: evidence that AtXRN4, one of several orthologs of nuclear Xrn2p/Rat1p, functions in the cytoplasm. Proc. Natl. Acad. Sci. USA *97*, 13985–13990.

Llave, C., Xie, Z., Kasschau, K.D., and Carrington, J.C. (2002). Cleavage of Scarecrow-like mRNA targets directed by a class of *Arabidopsis* miRNA. Science *297*, 2053–2056.

Lobbes, D., Rallapalli, G., Schmidt, D.D., Martin, C., and Clarke, J. (2006). SERRATE: a new player on the plant microRNA scene. EMBO Rep. *7*, 1052–1058.

Mallory, A.C., and Vaucheret, H. (2006). Functions of microRNAs and related small RNAs in plants. Nat. Genet. Suppl. *38*, S31–S36.

Mazza, C., Ohno, M., Segref, A., Mattaj, I.W., and Cusack, S. (2001). Crystal structure of the human nuclear cap binding complex. Mol. Cell *8*, 383–396.

Mi, S., Cai, T., Hu, Y., Chen, Y., Hodges, E., Ni, F., Wu, L., Li, S., Zhou, H., Long, C., et al. (2008). Sorting of small RNAs into *Arabidopsis* argonaute complexes is directed by the 5′ terminal nucleotide. Cell *133*, 116–127.

Olmedo, G., Guo, H., Gregory, B.D., Nourizadeh, S.D., Aguilar-Henonin, L., Li, H., An, F., Guzman, P., and Ecker, J.R. (2006). ETHYLENE-INSENSITIVE5 encodes a 5′→3′ exoribonuclease required for regulation of the EIN3-targeting F-box proteins EBF1/2. Proc. Natl. Acad. Sci. USA *103*, 13286–13293.

Onodera, Y., Haag, J.R., Ream, T., Nunes, P.C., Pontes, O., and Pikaard, C.S. (2005). Plant nuclear RNA polymerase IV mediates siRNA and DNA methylation-dependent heterochromatin formation. Cell *120*, 613–622.

Park, W., Li, J., Song, R., Messing, J., and Chen, X. (2002). CARPEL FACTORY, a Dicer homolog, and HEN1, a novel protein, act in microRNA metabolism in *Arabidopsis thaliana*. Curr. Biol. *12*, 1484–1495.

Parry, D.H., Xu, J., and Ruvkun, G. (2007). A whole-genome RNAi Screen for C. elegans miRNA pathway genes. Curr. Biol. *17*, 2013–2022.

Peragine, A., Yoshikawa, M., Wu, G., Albrecht, H.L., and Poethig, R.S. (2004). SGS3 and SGS2/SDE1/RDR6 are required for juvenile development and the production of trans-acting siRNAs in Arabidopsis. Genes Dev. *18*, 2368–2379.

Pontier, D., Yahubyan, G., Vega, D., Bulski, A., Saez-Vasquez, J., Hakimi, M.A., Lerbs-Mache, S., Colot, V., and Lagrange, T. (2005). Reinforcement of silencing at transposons and highly repeated sequences requires the concerted action of two distinct RNA polymerases IV in *Arabidopsis*. Genes Dev. *19*, 2030–2040.

Potuschak, T., Vansiri, A., Binder, B.M., Lechner, E., Vierstra, R.D., and Genschik, P. (2006). The exoribonuclease XRN4 is a component of the ethylene response pathway in *Arabidopsis*. Plant Cell *18*, 3047–3057.

Prigge, M.J., and Wagner, D.R. (2001). The *Arabidopsis* serrate gene encodes a zinc-finger protein required for normal shoot development. Plant Cell *13*, 1263–1279.

Qi, Y., Denli, A.M., and Hannon, G.J. (2005). Biochemical specialization within *Arabidopsis* RNA silencing pathways. Mol. Cell *19*, 421–428.

Qi, Y., He, X., Wang, X.J., Kohany, O., Jurka, J., and Hannon, G.J. (2006). Distinct catalytic and non-catalytic roles of ARGONAUTE4 in RNA-directed DNA methylation. Nature *443*, 1008–1012.

Rajagopalan, R., Vaucheret, H., Trejo, J., and Bartel, D.P. (2006). A diverse and evolutionarily fluid set of microRNAs in *Arabidopsis thaliana*. Genes Dev. *20*, 3407–3425.

Souret, F.F., Kastenmayer, J.P., and Green, P.J. (2004). AtXRN4 degrades mRNA in *Arabidopsis* and its substrates include selected miRNA targets. Mol. Cell *15*, 173–183.

Tomari, Y., and Zamore, P.D. (2005). Perspective: machines for RNAi. Genes Dev. *19*, 517–529.

Vaucheret, H., Vazquez, F., Crete, P., and Bartel, D.P. (2004). The action of ARGONAUTE1 in the miRNA pathway and its regulation by the miRNA pathway are crucial for plant development. Genes Dev. *18*, 1187–1197.

Vazquez, F., Gasciolli, V., Crete, P., and Vaucheret, H. (2004a). The nuclear dsRNA binding protein HYL1 is required for microRNA accumulation and plant development, but not posttranscriptional transgene silencing. Curr. Biol. *14*, 346–351.

Vazquez, F., Vaucheret, H., Rajagopalan, R., Lepers, C., Gasciolli, V., Mallory, A.C., Hilbert, J.L., Bartel, D.P., and Crete, P. (2004b). Endogenous trans-acting siRNAs regulate the accumulation of *Arabidopsis* mRNAs. Mol. Cell *16*, 69–79.

Willmann, M.R., and Poethig, R.S. (2007). Conservation and evolution of miRNA regulatory programs in plant development. Curr. Opin. Plant Biol. *10*, 503–511.

Xie, Z., Johansen, L.K., Gustafson, A.M., Kasschau, K.D., Lellis, A.D., Zilberman, D., Jacobsen, S.E., and Carrington, J.C. (2004). Genetic and functional diversification of small RNA pathways in plants. PLoS Biol. *2*, E104. 10.1371/journal.pbio.0020104.

Yang, L., Liu, Z., Lu, F., Dong, A., and Huang, H. (2006). SERRATE is a novel nuclear regulator in primary microRNA processing in Arabidopsis. Plant J. *47*, 841–850.

Yoshikawa, M., Peragine, A., Park, M.Y., and Poethig, R.S. (2005). A pathway for the biogenesis of trans-acting siRNAs in *Arabidopsis*. Genes Dev. *19*, 2164–2175.

Developmental Cell, volume 14

Supplemental Data

A Link between RNA Metabolism and Silencing Affecting Arabidopsis Development

Brian D. Gregory, Ronan C. O'Malley, Ryan Lister, Mark A. Urich, Julian Tonti-Filippini, Huaming Chen, A. Harvey Millar, and Joseph R. Ecker

SUPPLEMENTAL METHODS

Microarray Analysis

15 μg of total RNA isolated using the RNeasy Plant Mini Kit (Qiagen, Valencia, CA) from immature flower bud clusters was used for tiling microarray analysis as previously described (Chekanova et al., 2007; Zhang et al., 2006). Two biological replicates were performed for wild-type Col-0, *abh1-1*, *ein5-6*, and *ein5-6 abh1-1* mutant plants. To do this, oligo(dT)-primed targets prepared from wild-type (Col-0), *abh1-1*, *ein5-6* and *ein5-6 abh1-1* plants were hybridized to *Arabidopsis* tiling arrays. The tiling arrays used for this analysis were the Affymetrix® GeneChip® Arabidopsis Tiling 1.0F and GeneChip® Arabidopsis Tiling 1.0R Arrays, which are housed in the Gene Expression Omnibus (GEO) under the accessions GPL1979 and GPL1980, respectively (Zhang et al., 2006). We then employed the TileMap algorithm (Ji and Wong, 2005), which utilizes a two-state hidden Markov model based on probe-level t statistics, to identify genomic regions showing statistically significant expression changes between the mutant genotypes and wild-type Col-0 plants (Fig. S2 and Tables S1-S6). The Tilemap tiling array analysis was performed as previously described (Chekanova et al., 2007), with the exception that a posterior probability value of 0.6 was used.

smRNA library construction

Total RNA was isolated using the RNeasy Plant Mini Kit (Qiagen, Valencia, CA). Immediately following RNA precipitation, the flow through from the anion-exchange chromatography column was further precipitated in another 2.5 volumes of 100% ethanol (smRNA fraction). The smRNA fraction was further purified by a phenol-chloroform extraction and an additional ethanol precipitation. smRNAs were resolved by electrophoresis of 2.5 μg of the smRNA fraction and 7.5 μg of total RNA on 15% polyacrylamide gels containing 7 M urea in TBE buffer (45 mM Tris-borate, pH 8.0, and 1.0 mM EDTA). A gel slice containing RNAs of 15 to 35 nucleotides (based on the 10 base pair ladder size standard (Invitrogen, Carlsbad, CA)) was excised and eluted in 0.2 M NaCl rotating at room temperature for 4 hours. The eluted RNAs were precipitated using ethanol and resuspended in diethyl pyrocarbonate–treated deionized water. Gel-purified smRNA molecules were ligated sequentially to 5' and 3' RNA oligonucleotide adapters using T4 RNA ligase (10 units/μL) (Promega, Madison, WI). The 5' RNA adapter (5' - GUUCAGAGUUCUACAGUCCGACGAUC - 3') possessed 5' and 3' hydroxyl groups. The 3' RNA adapter (5' - pUCGUAUGCCGUCUUCUGCUUGidT - 3') possessed a 5' mono-phosphate

and a 3' inverted deoxythymidine (idT). All oligonucleotides (including RNA and DNA) were provided by Illumina (Illumina Inc., San Diego, CA). The smRNAs were first ligated to the 5' RNA adapter. The ligation products were gel eluted and ligated to the 3' RNA adapter as described above. The final ligation products were then used as templates in a reverse transcription (RT) reaction using the RT-primer (5' - CAAGCAGAAGACGGCATACGA - 3') and Superscript II reverse transcriptase (Invitrogen Inc., Carlsbad, CA). This was followed by a limited (16 cycle) PCR amplification step using the PCR reverse (5' – AATGATACGGCGACCACCGACAGGTTCAGAGTTCTACAGTCCGA - 3') and forward (5' - CAAGCAGAAGACGGCATACGA - 3') primers and Phusion hot-start high fidelity DNA polymerase (New England Biolabs, Cambridge, MA). The amplification products were electrophoresed on a 6% polyacrylamide gel in TBE buffer, eluted in 0.2 M NaCl rotating at room temperature for 4 hours, precipitated using ethanol, and resuspended in nuclease-free water. A schematic of this procedure is presented in Figure S3.

GMUCT sequencing library construction

Total RNA from wild-type Col-0 and *ein5-6* immature flower buds was isolated using the RNeasy Plant Mini Kit (Qiagen, Valencia, CA) and treated with Rnase-free DNaseI (Qiagen) for 25 min at room temperature. Following an ethanol precipitation, poly(A)$^+$ RNA was column purified from 50 μg of the total RNA samples using Oligotex mRNA kit (Qiagen). The poly(A)$^+$ RNA was then depleted for18S and 28S rRNA molecules in two sequential Ribominus (Invitrogen, Carlsbad, CA) reactions as per manufacturer's instructions, using 6 plant-specific biotinylated LNA oligonucleotide rRNA probes supplied by the manufacturer (Invitrogen, Carlsbad, CA). The rRNA-depleted poly(A)$^+$ RNA was then ligated to the Illumina 5' smRNA adapter using T4 RNA ligase (10 units/μL) (Promega, Madison, WI). The 5' RNA adapter (5' - GUUCAGAGUUCUACAGUCCGACGAUC - 3') possessed 5' and 3' hydroxyl groups. The ligated rRNA-depleted poly(A)$^+$ RNA was purified by phenol:chloroform extraction and ethanol precipitation. Oligo(dT) was then used to prime cDNA synthesis using SuperScript II reverse transcriptase(200 units/μL) (Invitrogen, Carlsbad, CA). The cDNA was then subjected to second strand synthesis using Oligo(dT) and the PCR primer specific for the Illumina 5' smRNA adapter (5' – AATGATACGGCGACCACCGACAGGTTCAGAGTTCTACAGTCCGA - 3'). The dscDNA was ethanol precipiated, and then fragmented by sonication to 50-500 bp with a Bioruptor (Diagenode Sparta, NJ), followed by end repair and ligation of the genomic DNA (gDNA) adapters provided by Illumina (Illumina, San Diego, CA) as per manufacturer's instructions for gDNA library construction. 100-200 ng of adapter-ligated dscDNA of 195-235 bp was isolated by agarose gel electrophoresis, and subsequently purified using a gel extraction kit (Qiagen, Valencia, CA). This was followed by a limited (16 cycle) PCR amplification step using the PCR primer specific for the Illumina 5' smRNA adapter (5' – AATGATACGGCGACCACCGACAGGTTCAGAGTTCTACAGTCCGA - 3') and

primer 2.1 that is specific for the gDNA 3' adapter using Phusion hot-start high fidelity DNA polymerase (New England Biolabs, Cambridge, MA). Using this primer combination for the limited amplification enriched for the desired products that had an Illumina 5' smRNA adapted on the 5' end and the 3' gDNA adapter on the 3' end. The enriched library was purified with the PCR purification kit (Qiagen, Valencia, CA) and quantity and quality examined by spectrophotometry, gel electrophoresis, and limited sequencing of cloned library molecules. A schematic of this procedure is presented in Figure S12.

SUPPLEMENTAL REFERENCES

Chekanova, J. A., Gregory, B. D., Reverdatto, S. V., Chen, H., Kumar, R., Hooker, T., Yazaki, J., Li, P., Skiba, N., Peng, Q*., et al.* (2007). Genome-wide high-resolution mapping of exosome substrates reveals hidden features in the Arabidopsis transcriptome. Cell *131*, 1340-1353.

Ji, H., and Wong, W. H. (2005). TileMap: create chromosomal map of tiling array hybridizations. Bioinformatics *21*, 3629-3636.

Zhang, X., Yazaki, J., Sundaresan, A., Cokus, S., Chan, S. W., Chen, H., Henderson, I. R., Shinn, P., Pellegrini, M., Jacobsen, S. E., and Ecker, J. R. (2006). Genome-wide high-resolution mapping and functional analysis of DNA methylation in arabidopsis. Cell *126*, 1189-1201.

SUPPLEMENTAL FIGURES

Figure S1. *ein5* mutant plant developmental defects are enhanced by *abh1* mutation. (A-D) Flowers of wild type Col-0 (A), *abh1-1* (B), *ein5-6* (C), and *ein5-6 abh1-1* (D) plants. *ein5-6 abh1-1* double mutant flowers also manifested defects not observed for either single mutant or wild-type Col-0; including extranumerary petals and bending of the gynoecium.

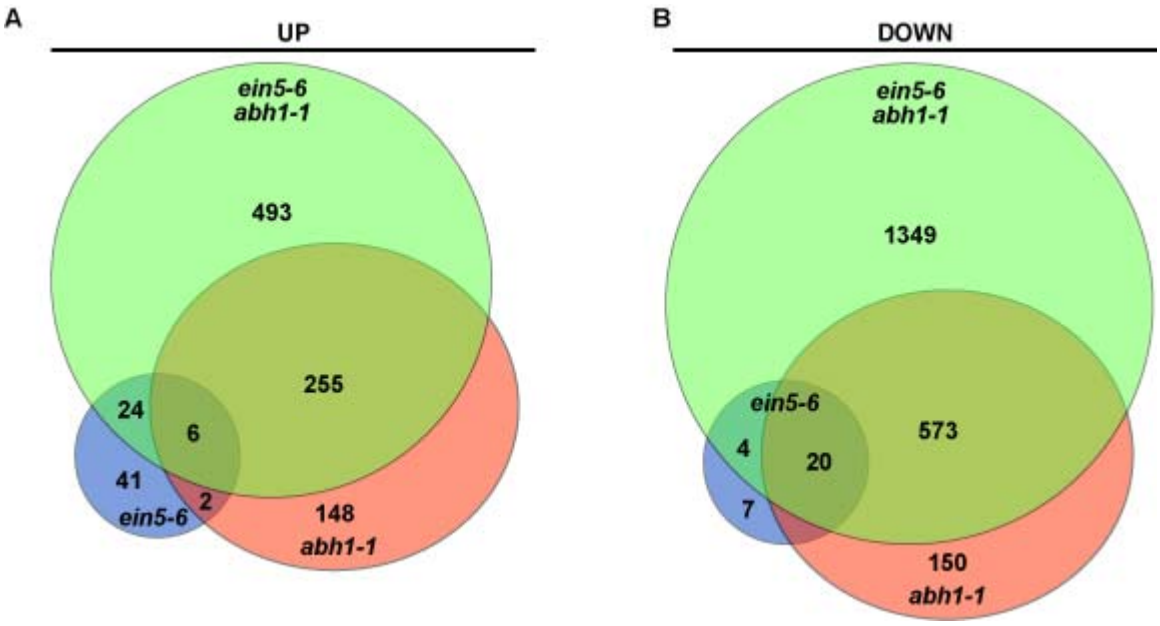

Figure S2. Venn diagram representation of tiling microarray analysis demonstrating the up and down-regulated expression changes in the Arabidopsis transcriptome in response to mutation of *ABH1* and/or *EIN5*. Some of the more interesting up-regulated targets for *abh1-1* (primary *MIRNA* transcripts (Fig. 3)) and *ein5-6 abh1-1* (primary *MIRNA* transcripts and miRNA target mRNAs (Fig. 3)) double mutant plants are highlighted in Figure 3.

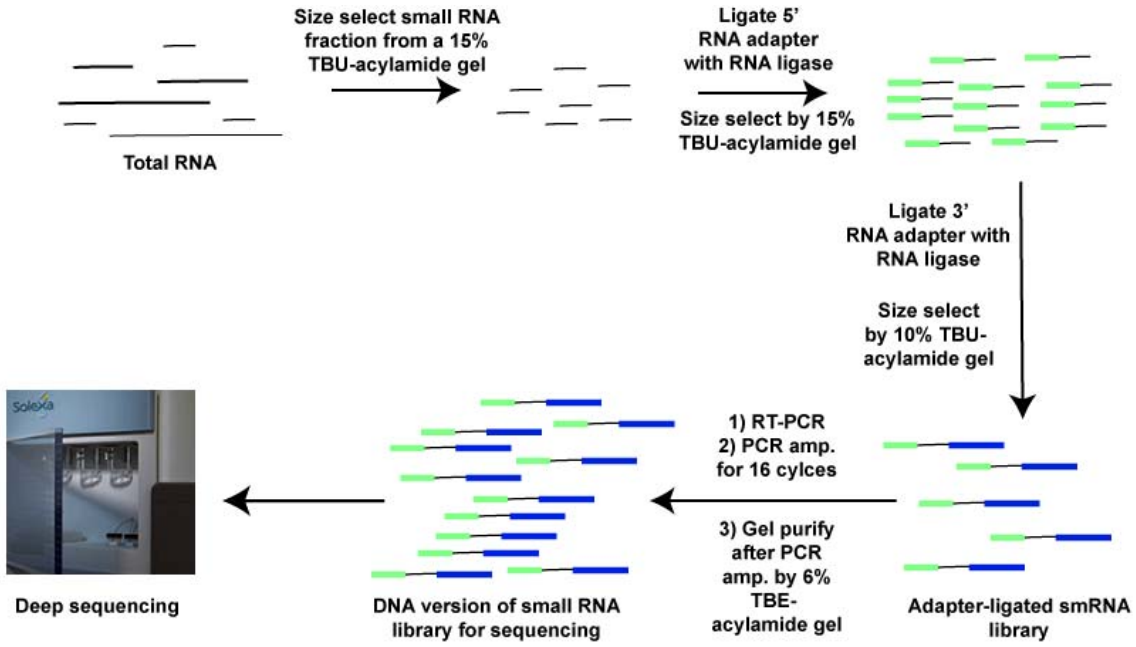

Figure S3. Schematic of deep sequencing of the smRNA-component of the transcriptome using an Illumina Genetic Analyzer. See Supplemental Methods for details on methodology.

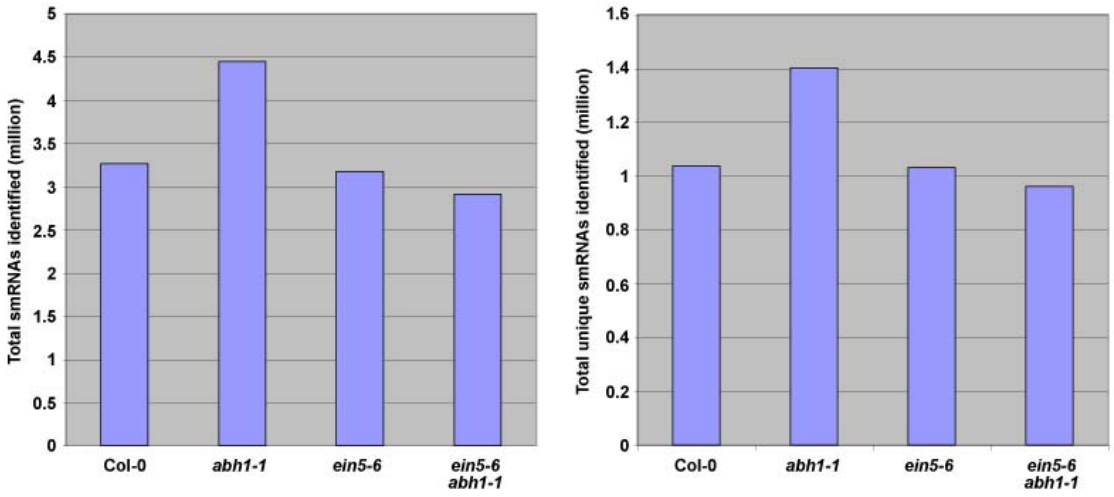

Figure S4. Deep sequencing of smRNAs from wild-type Col-0, *abh1-1*, *ein5-6*, and *ein5-6 abh1-1* double mutant plants using an Illumina Genetic Analyzer. (A) The total number of smRNAs identified from Illumina smRNA libraries of wild-type Col-0, *abh1-1*, *ein5-6*, and *ein5-6 abh1-1* double mutant plants. (B) The number of smRNAs with completely unique 5' ends identified from Illumina smRNA libraries of wild-type Col-0, *abh1-1*, *ein5-6*, and *ein5-6 abh1-1* double mutant plants.

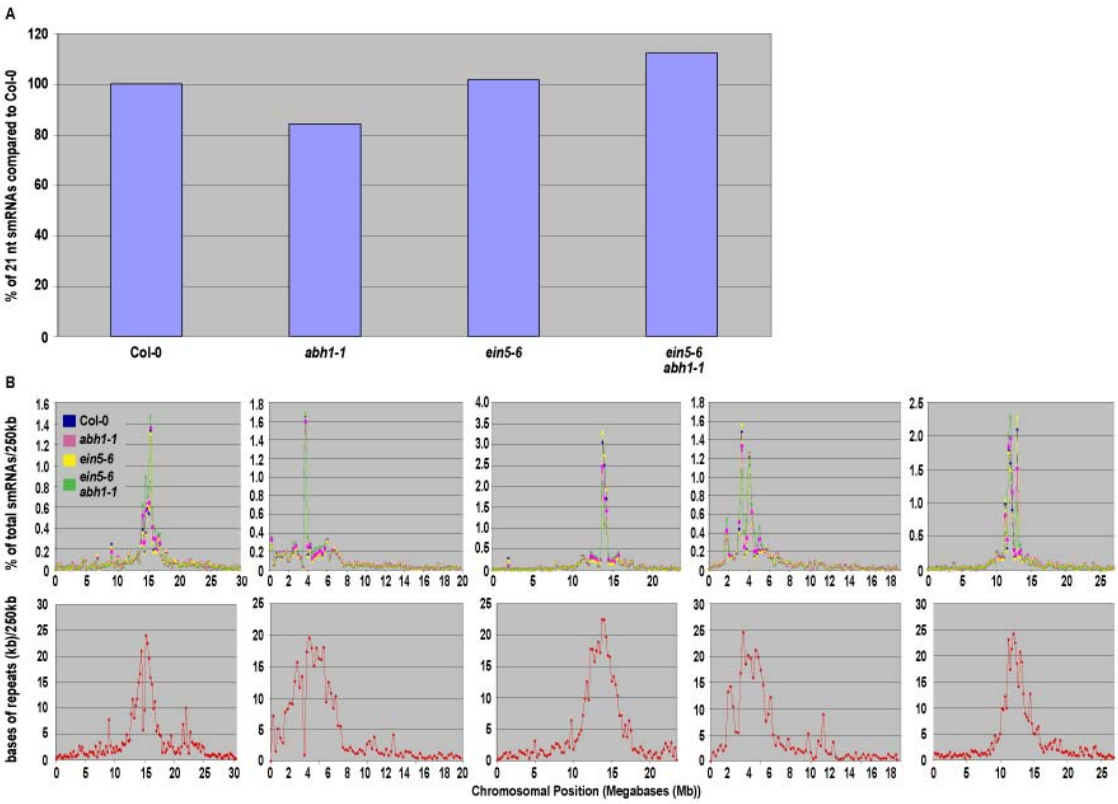

Figure S5. Deep sequencing of smRNA populations from wild-type Col-0, *abh1-1*, *ein5-6*, and *ein5-6 abh1-1* mutant plants demonstrates that ABH1 is required for proper accumulation of numerous highly abundant 21 nt smRNAs, while concomitant loss of ABH1 and EIN5 results in the accumulation of distinct 21 nt smRNAs. (A) The percent of total reads (with wild-type Col-0 being set at 100%) corresponding to 21 nt smRNAs from wild-type Col-0, *abh1-1*, *ein5-6*, and *ein5-6 abh1-1* double mutant plants. *abh1-1* mutant plants accumulate significantly fewer 21 nt smRNAs compared to wild-type Col-0, whereas *ein5-6 abh1-1* double mutant plants demonstrate an expansion of this class of smRNAs. (B) The top panels demonstrate the normalized abundance of 24 nt smRNAs (*y* axis, left-side scale) in a sliding 250 kb window in wild-type (Col-0) (blue line), *abh1-1* (pink line), *ein5-6* (yellow line), and *ein5-6 abh1-1* (green line) double mutant plants. The bottom panels demonstrate the total lengths (base pairs) of all repeats in a sliding 250 kb window.

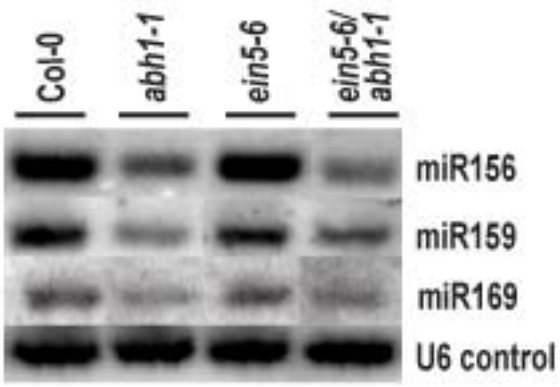

Figure S6. ABH1 is required for proper miRNA processing. SmRNA northern blot analysis of samples from indicated genotypes with DNA probes complementary to miRNA156, 159, and 169. U6 is shown as a loading control.

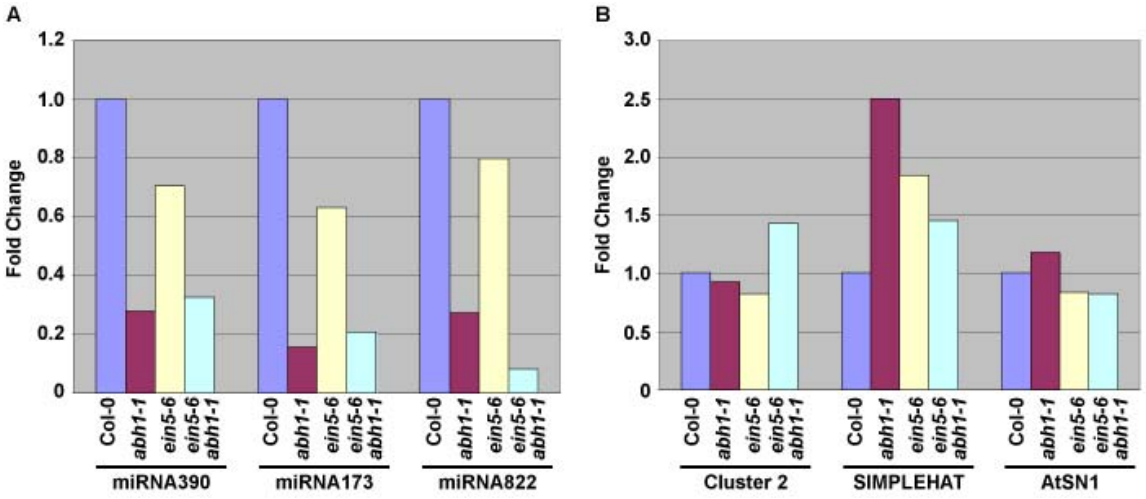

Figure S7. ABH1 is required for proper miRNA processing. (A) Normalized values of specific miRNAs to total read numbers (Figure S4) obtained by smRNA sequencing with an Illumina GA for the indicated genotypes. (B) Normalized values of specific heterochromatic smRNAs (24 nt smRNA sequences) for the indicated genotypes. In Figure S7A, we show data for miRNA390 to serve as control for a miRNA that was also validated as being reduced in the absence of ABH1 function by smRNA northern blotting (Figure 4B-C). Specifically, the comparison of results presented in Figure S7A to those in Figure 4B-C demonstrates that the quantitation of miRNA390 levels from the sequencing data are very similar to those obtained from northern blot analysis. Therefore, quantitation of the effects of ABH1 and/or EIN5 on the levels of other miRNAs for which northern blots are not available (miRNA 173 and 822 shown) can also be extracted from the smRNA sequencing data. Overall, the collection of smRNA sequences we present here provides a vast set of data from which the effects of ABH1 and/or EIN5 on various populations of smRNAs can be determined quantitatively.

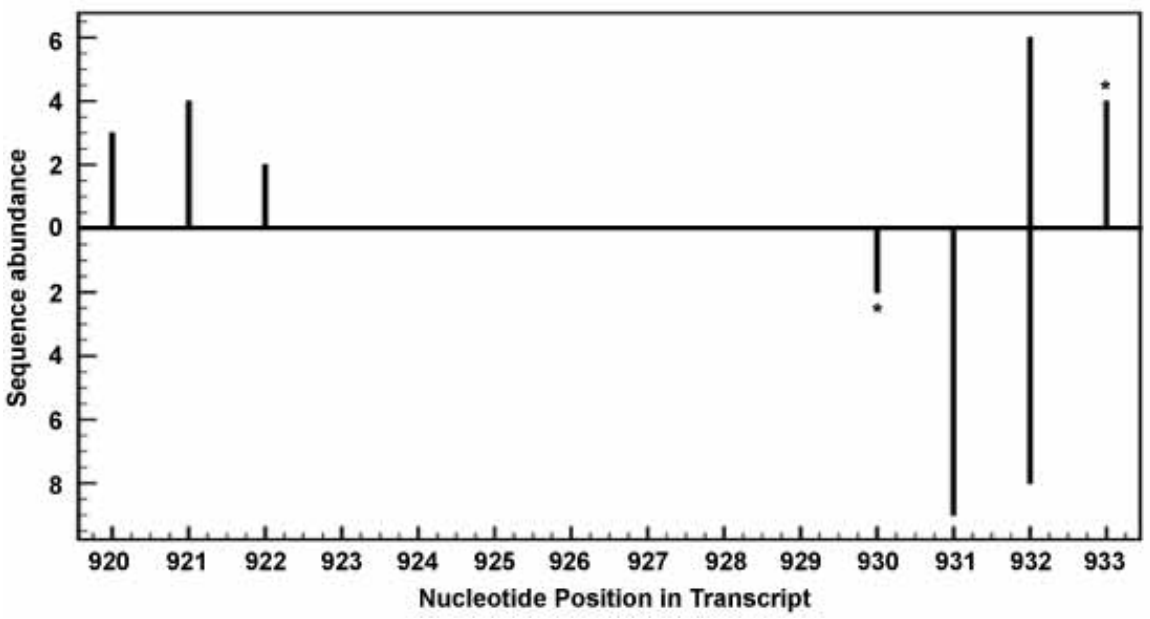

Figure S8. The number of smRNA reads with a 5' terminus at each position is plotted for smRNAs processed from the 3' end of *At3g46550* (bp 920 to 933). Bars above the axis represent sense reads; below represent antisense reads. The tick marks denote a single nucleotide position within the transcript. The two asterisks denote phased siRNAs originating from the sense (nt 933) and antisense (930) strands, while taking into account the 2 nt overhang that is likely to be a byproduct of processing of these smRNAs. Most strikingly, this analysis demonstrated that EIN5-affected smRNAs are processed in multiple 21 nt registers. This 13 nt stretch of *At3g46550* is used as a model for what is also demonstrated for the processing of EIN5-affected smRNAs from the other 133 loci (Supplemental Tables S11-12). Specifically, we find that for all EIN5-affected smRNA-generating loci processing of this class of smRNAs occurs from multiple 21 nt registers for some of which we can identify phased siRNAs. Overall, this analysis suggests that there is not an ordered processing event or "common" mRNA terminus that is consistently required for biogenesis of these smRNAs.

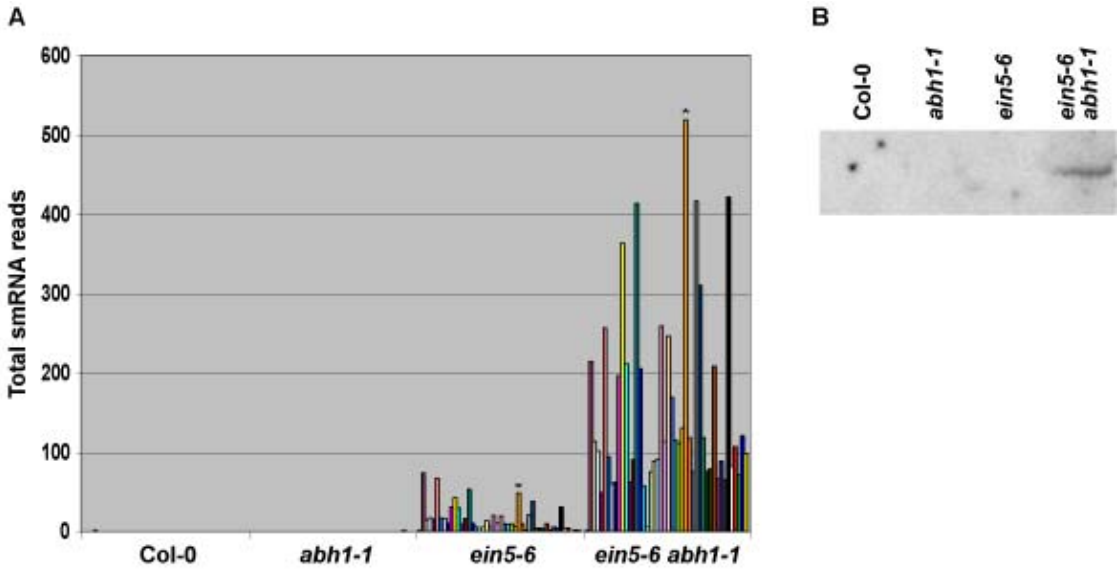

Figure S9. SmRNA Northern blot analysis of EIN5-affected smRNAs. (A) The graph shows the total amount of smRNA reads emanating from all positions of the *At5g65630* transcript. The asterisk above one of the graph bars marks the smRNA that is interrogated in the blot in panel. B. Interestingly, low levels of one of these smRNAs can be detected in the wild-type Col-0 sample, which suggests that they are processed in wild-type *Arabidopsis* plants. (B) RNA gel-blot analyses of smRNA-enriched RNA isolated from unopened flower clusters of wild-type Col-0, *abh1-1*, *ein5-6*, and *ein5-6 abh1-1* double mutant plants with DNA probes complementary to the smRNA marked by an asterisk in A. *ein5-6 abh1-1* double mutant plants accumulate sufficient levels of this EIN5-affected smRNA to be detected by our Northern blot analysis. It is likely that the levels of this smRNA in *ein5-6* mutant plants are below the limit of detection in that these single mutant plants accumulate ~5-fold lower levels than double mutant plants.

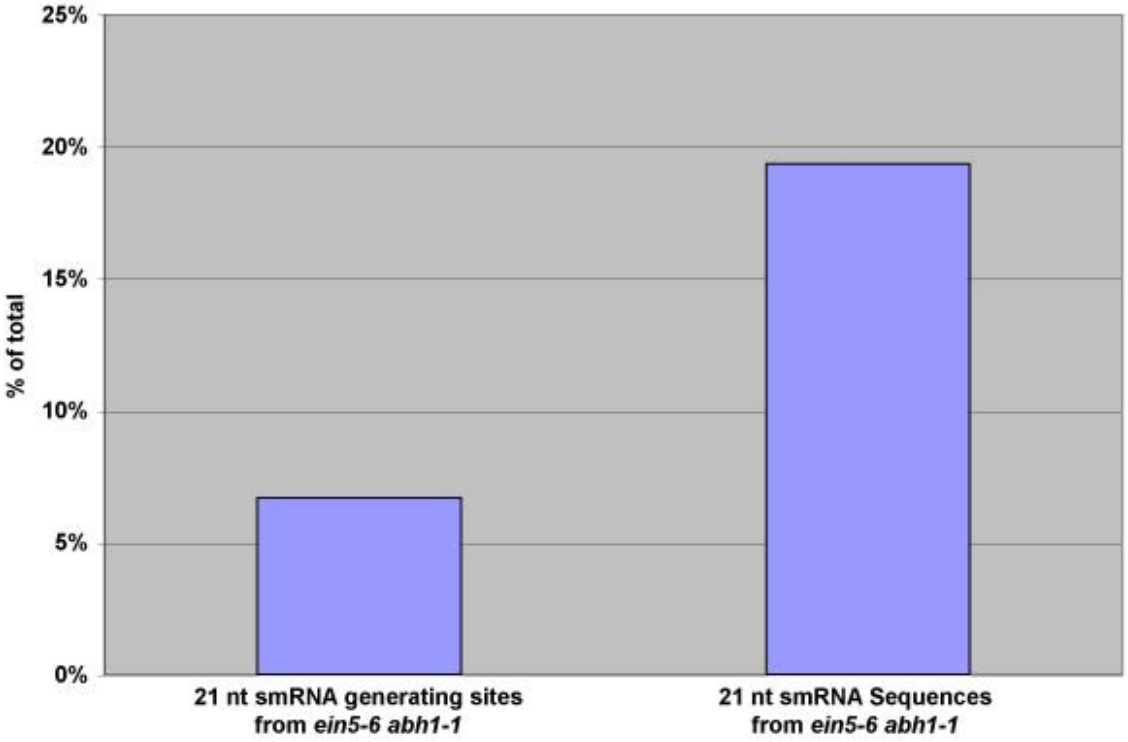

Figure S10. EIN5-affected smRNAs become a significant proportion of the 21 nt smRNA population in *ein5-6 abh1-1* double mutant plants. The graph shows the percent of total 21 nt smRNA-generating sites occupied by EIN5-affected smRNAs in *ein5-6 abh1-1* double mutant plants (left bar). Additionally, the graph shows the percent of all 21 nt smRNA sequenced reads occupied by EIN5-affected smRNAs in *ein5-6 abh1-1* double mutant plants (right bar). Surprisingly, this class of smRNAs makes up ~19% of the total population of 21 nt smRNAs sequenced from *ein5-6 abh1-1* double mutant plants, which suggests that the expansion of EIN5-affected smRNAs could dilute the other populations of 21 nt smRNAs.

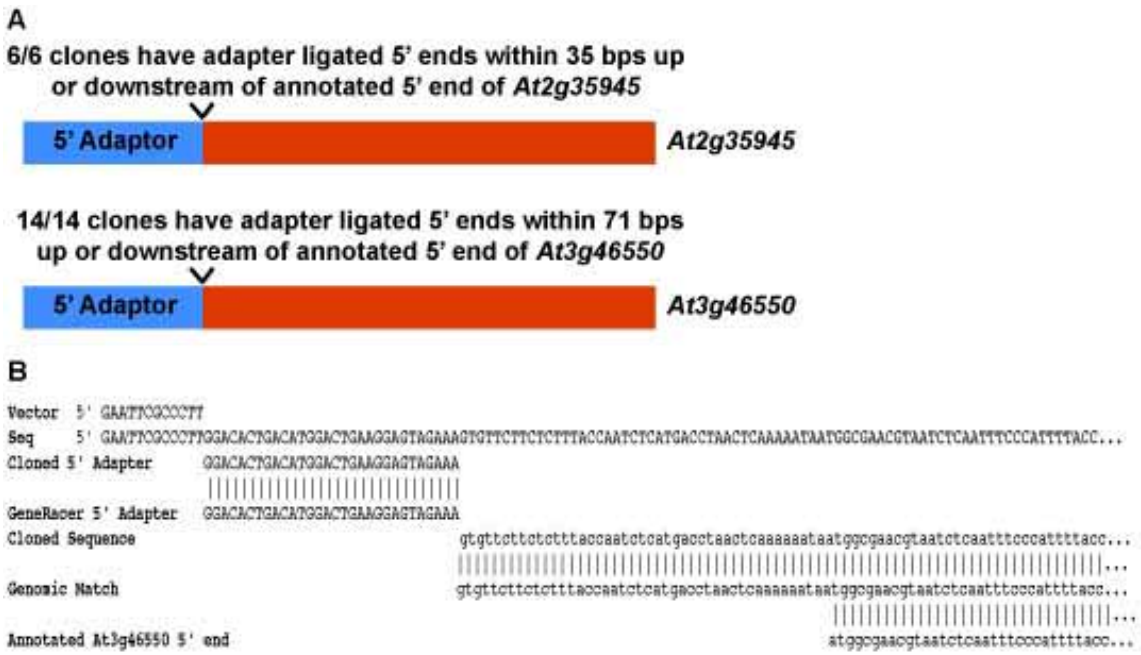

Figure S11. Transcripts from which EIN5-affected smRNAs are processed accumulate in an uncapped form. (A) Products from 5' RACE reactions (Fig. 6A) were cloned and sequenced. All six clones sequenced from the 5' RACE reactions for *At2g35945* contained sequence abutting the 5' RNA adapter that was within 35 bp up or downstream of the annotated 5' end of this transcript. Additionally, all 14 clones sequenced from the 5' RACE reactions for *At3g46550* contained sequence abutting the 5' RNA adapter that was within 71 bp up or downstream of the annotated 5' end of this transcript. Interestingly, the cloned sequence that mapped furthest from the annotated 5' end was homologous to sequence that started 71 bp of upstream of this site. (B) This is an example of one of the cloned 5' RACE products for *At3g46550*, where the RNA adapter was directly ligated to RNA that is homologous to this transcript starting 43 bp upstream of the annotated 5' end. In fact, 3/14 cloned products consisted of this exact same adapter-ligated product.

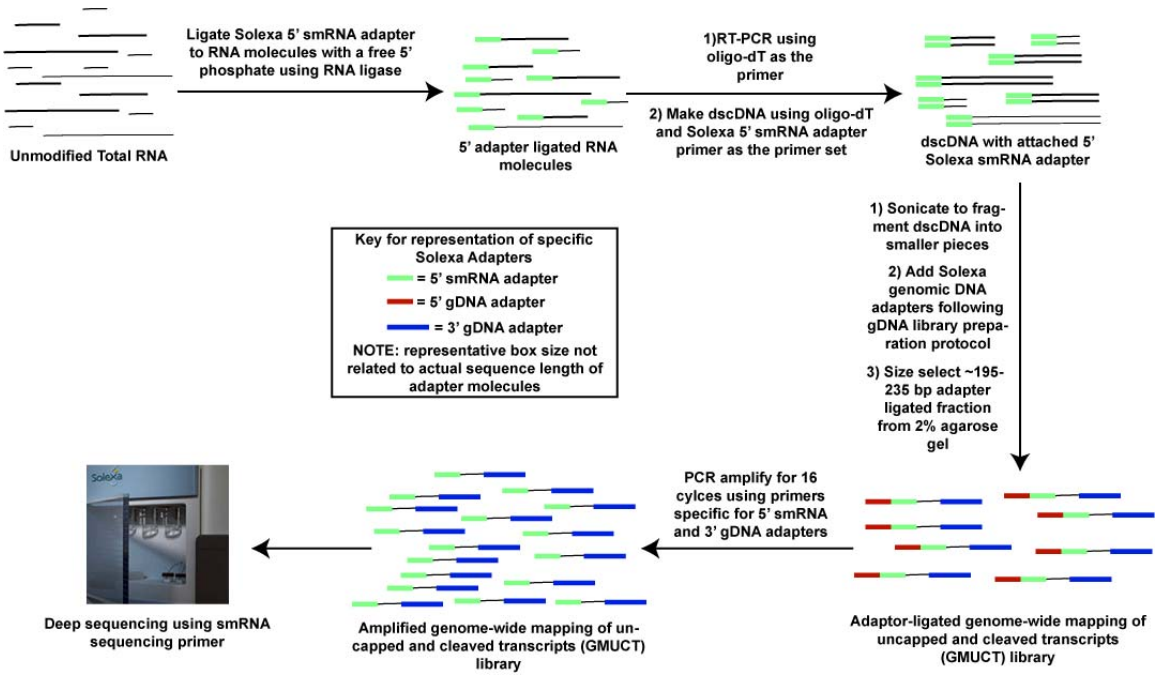

Figure S12. Schematic of extremely deep sequencing of genome-wide mapping of uncapped and cleaved transcript (GMUCT) libraries using an Illumina Genetic Analyzer. See supplemental materials and methods for details on methodology.

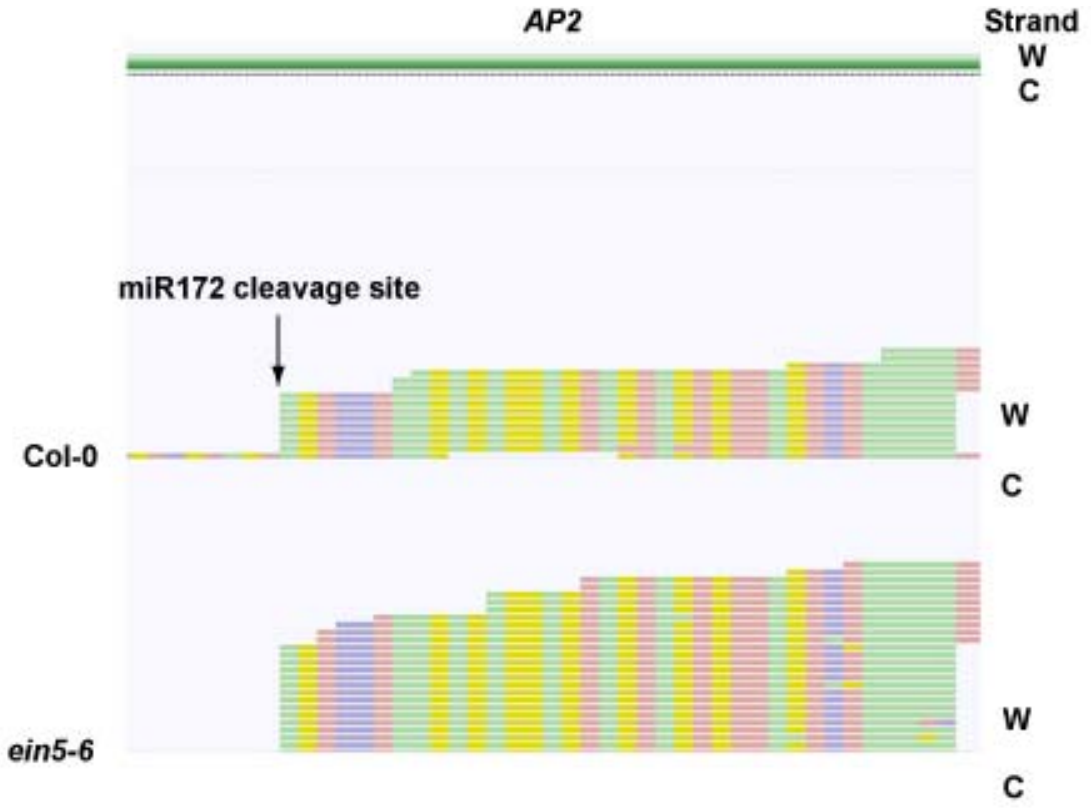

Figure S13. An example of a miRNA-mediated target mRNA cleavage site (screenshots from the smRNAome database) that was determined using the GMUCT method, which provides validation that this methodology is identifying the expected substrates. W and C indicate signal from Watson and Crick strands, respectively. Multi-colored bars represent independent Illumina sequencing reads. For the sequencing data the color coding is as follows: green = T, red = A, yellow = C, and blue = G.

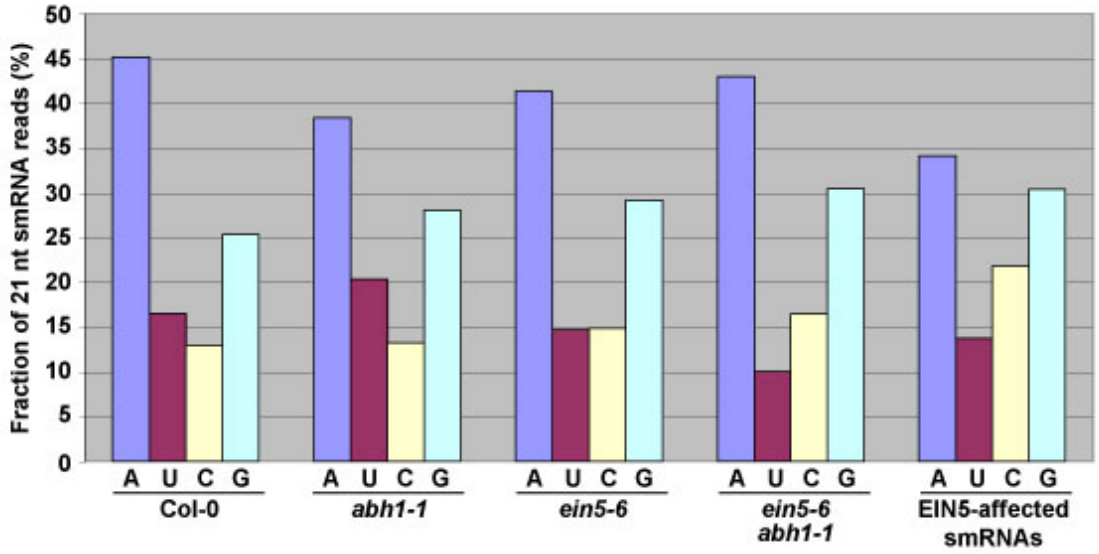

Figure S14. The relative frequencies of each of the four nucleotides (A, U, C, G) as the 5' terminal nucleotide within the total population of 21 nt small RNAs from wild-type Col-0, *abh1-1*, *ein5-6*, *ein5-6 abh1-1*, and EIN5-affected smRNA generating loci specifically (all 133 loci were used for this analysis). This analysis demonstrated that there is not a significant difference in the 5' terminal nucleotide distribution within the total 21 nt smRNA populations from wild-type Col-0, *abh1-1*, *ein5-6*, *ein5-6/abh1-1* plants. Furthermore, the 5' terminal nucleotide distribution within the 21 nt EIN5-affected smRNA population is not significantly different from that of the total population of 21 nt smRNAs.